Mon. Not. R. Astron. Soc. **337,** 578–596 (2002)

Orbital dynamics of three-dimensional bars – III. Boxy/peanut edge-on profiles

P. A. Patsis,[1⋆] Ch. Skokos[1,2] and E. Athanassoula[3]

[1]*Research Centre of Astronomy, Academy of Athens, Anagnostopoulou 14, GR-10673 Athens, Greece*
[2]*Division of Applied Analysis, Department of Mathematics and Centre for Research and Application of Nonlinear Systems (CRANS), University of Patras, GR-26500, Patras, Greece*
[3]*Observatoire de Marseille, 2 Place Le Verrier, F-13248 Marseille, Cedex 4, France*

Accepted 2002 August 5. Received 2002 August 2; in original form 2002 May 2

ABSTRACT

We present families, and sets of families, of periodic orbits that provide building blocks for boxy and peanut (hereafter b/p) edge-on profiles. We find cases where the b/p profile is confined to the central parts of the model and cases where a major fraction of the bar participates in this morphology. A b/p feature can be built either by 3D families associated with 3D bifurcations of the x1 family, or, in some models, even by families related with the z-axis orbits and existing over large energy intervals. The 'X' feature observed inside the boxy bulges of several edge-on galaxies can be attributed to the peaks of successive x1v1 orbits, provided their stability allows it. However in general, the x1v1 family has to overcome the obstacle of a $S \rightarrow \Delta \rightarrow S$ transition in order to support the structure of a b/p feature. Other families that can be the backbones of b/p features are x1v4 and z3.1s. The morphology and the size of the boxy or peanut-shaped structures we find in our models are determined by the presence and stability of the families that support b/p features. The present study favours the idea that the observed edge-on profiles are the imprints of families of periodic orbits that can be found in appropriately chosen Hamiltonian systems, describing the potential of the bar.

Key words: galaxies: evolution – galaxies: kinematics and dynamics – galaxies: structure.

1 INTRODUCTION

Disc galaxies, when observed edge-on, often exhibit a box- or peanut-like structure. As this is confined to the inner parts of the galaxy, and because it extends in the vertical direction outside the disc, this structure has been called a boxy or peanut (hereafter b/p) bulge. Yet there are many ways in which it differs from ordinary bulges. The b/p structures have their maximum thickness not at the centre of the galaxy, like in usual $R^{1/4}$ spheroids, but 'at two points symmetrically spaced on either side of the centre' (Burbidge & Burbidge 1959). Another difference from $R^{1/4}$-bulges and ellipticals is that b/p structures rotate 'cylindrically', i.e. their observed rotation is independent of the height above the plane, whereas bulges and ellipticals do not (e.g. Kormendy & Illingworth 1982). There is one more characteristic of b/p features related to their kinematics: Kuijken & Merrifield (1995) and Bureau & Freeman (1999) have shown that there are important differences between the position velocity diagrams of b/p structures and those of bulges. These have been used by Bureau & Athanassoula (1999) and Athanassoula & Bureau (1999) to develop diagnostics to detect the presence and orientation of a bar in edge-on disc galaxies. The method relies on the presence of x2 orbits in the bars of the galaxies. Having seen these differences, we will avoid calling the b/p features 'bulges', unless we are referring to particular observations.

Recent statistical studies (Lütticke, Dettmar & Pohlen 2000a) using 1350 galaxies from the RC3 show that 45 per cent of the profiles of edge-on disc galaxies are box- or peanut-shaped. Observational studies (e.g. Bureau & Freeman 1999; Lütticke, Dettmar & Pohlen 2000b) associate the b/p structure with the presence of a bar. Lütticke et al. (2000b) classify the bulges according to their boxiness and conclude that galaxies with a prominent b/p shape have a large BAL/BUL ratio, where BAL is the projected bar length, and BUL the bulge length. Photometrically isolating the b/p structure from the bulge, they measure the ratio of the projected bar length to the length of the b/p structure (BAL/BPL). Unfortunately this is only achieved for six galaxies, and gives an average value of 2.7 ± 0.4. This ratio indicates a structure confined close to the centre of the galaxy.

Bars and edge-on b/p morphology are linked in all the above mentioned papers, as well as in many others. However, the percentage of the bar which takes part in the b/p structure, i.e. whether we have a b/p feature on top of the bar, or whether we have a b/p-shaped bar in total, is an open question. The morphological differences

⋆E-mail: ppatsis@cc.uoa.gr

encountered among the various b/p features remains also to be explained.

In a few cases (e.g. IC 4767, Hickson 87a) an 'X'-shaped structure is found to be embedded in a boxy structure. It differs from the usual peanut in that the branches of the 'X' feature resemble segments of nearly straight lines that give the impression of intersecting each other. On the contrary, the classical peanuts have typically much rounder isophotes (see e.g. Shaw 1993) and, even in cases where these isophotes come very close to the equatorial plane of the galaxy at the centre, the visual impression is better described by the symbol '⊃⊂' than by an 'X' central morphology.[1] Lütticke, Dettmar & Pohlen (2000c), studying a sample of b/p galaxies including cases with 'X' features, estimated the angle between one branch of the 'X' and the major axis to be around $40^\circ \pm 10^\circ$. Studies of individual galaxies give for this angle values ranging from 22° for IC 4767 (Whitmore & Bell 1988) to 45° for NGC 128 (D'Onofrio et al. 1999). Pfenniger & Friedli (1991), taking as an example the case of IC 4767, claim that this feature is an optical illusion obtained when one uses a particular look-up-table for viewing the image. This view, however, is not generally shared. Thus Mihos, Walker & Hernquist (1995) used the process of 'unsharp masking' to enhance the 'X' embedded in the bulge of the galaxy Hickson 87a in order to compare this morphology with their model. In any case one can speak about characteristic kinks of the isophotes in edge-on profiles of a few galaxies and of the corresponding isodensities in snapshots of some *N*-body simulations (Athanassoula & Misiriotis 2002), which are aligned in such a way as to describe an 'X'-shaped feature.

There have been two approaches for explaining edge-on b/p profiles. The first invokes internal reasons, such as disc or orbital instabilities, and the second one invokes external reasons, such as encounters with companions, soft merging etc.

Combes & Sanders (1981) were the first to reproduce a b/p profile in *N*-body simulations of barred galaxies. Such structures have since then been found in many other simulations (e.g. Combes et al. 1990; Raha et al. 1991; Athanassoula & Misiriotis 2002) and are now considered a standard development in bar–unstable disc simulations. Pfenniger (1984a, 1985) associated the b/p morphology with the instability of the x1 family at the 4 : 1 vertical resonance. Later, Combes et al. (1990) suggested that the b/p shapes are due to the vertical 2 : 1 resonance, stressing the importance of having $\Omega_b = \Omega - \kappa/2 = \Omega - \nu/2$. This mechanism invokes a conjunction of the two resonances, i.e. the radial inner Lindblad resonance (radial ILR) and the vertical 2 : 1 resonance (v-ILR), and relates it to the appearance of a b/p edge-on morphology. The 3D families introduced at higher order resonances exist typically over smaller energy intervals and thus are less probable to be populated by orbits to build the box, although in principle they could be used as well. In such a case of course, they will support a thin morphological feature extending to large distances from the centre, i.e. close to corotation. The 2 : 1 vertical resonance is proposed as explanation of boxy structures also by Pfenniger & Friedli (1991), who speak about thick b/p bars. We mention that b/p features have also been found in edge-on profiles of orbital models of *normal* spiral galaxies with thick, 3D spirals embedded in discs (Patsis & Grosbøl 1996). Berentzen et al. (1998) have shown that a peanut shape may disappear when there is substantial gas inflow to the centre of the galaxy.

Building the peanut by accretion of material from satellite galaxies has been proposed initially by Binney & Petrou (1985), while Mihos et al. (1995) describe an encounter which produces the 'X' feature in the galaxy Hickson 87a. However, even in the cases where a companion is involved, the families of orbits that trap the infalling gas have to be studied.

In the present paper we investigate the vertical structure of bars using orbital theory. We do not construct self-consistent models, but we explore changes that occur when the main parameters of the system vary. We combine families of periodic orbits found in the models of Skokos, Patsis & Athanassoula (2002a, hereafter Paper I) and in the models of Skokos, Patsis & Athanassoula (2002b, hereafter Paper II), in order to build b/p features in the edge-on profiles. We also compare the geometry and the dimensions of the resulting systems with the corresponding features of edge-on galaxies. Speaking about a 'bulge' in the profiles of our models, we refer to a central enhancement of the density due to 3D orbits in our total potential. As we will see, the families of orbits we use are mainly 3D bifurcations of the planar x1 orbits, i.e. related to the families of the x1-tree that make the 3D bar in our models.

The layout of this paper is as follows: in Section 2 we describe the method we used to construct the vertical profiles of the families in the models and in Sections 3 and 4 we describe the properties of these profiles and the effect of combining several families together on the morphology of the models. In Section 5 we discuss our results and compare them with observations found in the literature, and finally in Section 6 we list our conclusions.

2 METHOD

2.1 The families of periodic orbits

Our general model consists of a Miyamoto disc, a Plummer bulge and a Ferrers bar. The total mass of the Miyamoto disc is M_D, and its horizontal and vertical scalelengths are A and B respectively. We have taken in all models $A = 3$ and $B = 1$. The total mass of the Plummer bulge is M_S and its scalelength ϵ_s. The mass of the Ferrers bar component is indicated by M_B and its semi-axes by a, b and c, where $a : b : c = 6 : 1.5 : 0.6$. The masses of the three components satisfy $G(M_D + M_S + M_B) = 1$, where G is the gravitational constant. The unit length is taken as 1 kpc, the unit time 1 Myr and the unit mass 2×10^{11} $M_\odot$. Details can be found in section 3.1 of Paper I, while the values of the parameters characterizing each particular model are given in the tables in the corresponding sections of the present paper.

In Papers I and II we calculated the families of periodic orbits which are the building blocks of 3D bars. Paper I presents the x1-tree in a fiducial case and the typical orbital behaviour of 3D bars in detail, while Paper II describes the differences observed in the orbital structure when the main parameters of the model vary. These papers also give the morphology of the orbits of each family. For the purpose of the present paper we are interested in the edge-on (side-on and end-on[2]) structures supported by the families, when one considers them as dynamical blocks. In this section we briefly review the properties of the main families we will discuss below. Throughout the paper the bar major axis lies along the y-axis and the axis of rotation is the z-axis.

(i) x1v1. In most of the models this is the first stable simple-periodic vertical bifurcation of x1, i.e. it bifurcates at the lowest energy at which the stability index associated with the vertical

[1] Nice examples can be found in the web page of L. Kuchinski at http://www.astronomy.ohio-state.edu/~lek/galx.html

[2] In the side-on view the line of sight is along the minor axis of the bar and in the end-on view it is along the major axis.

perturbations becomes $\leqq -2$. It is related to the 2 : 1 vertical resonance and both its (x, z) and (y, z) projections can be described as 'frowns' ('$\frown$') and 'smiles' ('$\smile$'). Several papers associate this family with the b/p bulges by combining its two branches which are symmetric with respect to the equatorial plane (Combes et al. 1990; Pfenniger & Friedli 1991). In many cases this family has a complex unstable part close to the energy at which it bifurcates from x1 (for an extensive description of complex instability in galactic potentials see e.g. Zachilas 1993).

(ii) x1v3. It is the stable 3D bifurcation of the models at the vertical 3 : 1 resonance. It is one of the standard building blocks of the 3D bar. Its (x, z) projection has a tilde-like shape '$(\sim)$', while the (y, z) one is a kind of a 'ooo' figure.

(iii) x1v4. This family is bifurcated as unstable from x1, also at the vertical 3 : 1 resonance region, but in many models it has large stable parts for larger energies. Thus it frequently is an important family of the system. Its (x, z) projection resembles the (y, z) projection of x1v3, i.e. it is a 'ooo' figure, while the (y, z) one has a tilde-like shape.

(iv) x1v5. It is bifurcated at the vertical 4 : 1 resonance. Both its edge-on projections can be morphologically described with the letter 'w', and it was the first family proposed for building the peanut (Pfenniger 1984a, 1985). In some models we have two x1v5-like families.

(v) z3.1s. This family is important in the model which lacks an explicit Plummer sphere bulge component in the potential. Morphologically it resembles the x1v4 family, but it is not related to the x1-tree.

(vi) x2-like 3D families. Finally, in a couple of cases, we found stable 3D x2-like families, i.e. families whose (x, y) projections have elliptical-like shapes elongated along the bar *minor* axis. They are bifurcations from the planar x2 orbits.

We note that all families have counterparts which are symmetric with respect to the principal planes and one can take into account all these orbits in order to build a profile. The rest of the stable 3D families found in Papers I and II also contribute to the vertical profiles of the models, but play a less important role. In Section 3, we refer to some of them in the description of the profiles of each model.

2.2 The weights of the orbits

In order to estimate the edge-on morphologies that can be supported we use, as a tool, profiles built by sets of weighted periodic orbit. For this we first calculate a set of stable periodic orbits and pick points along each orbit at equal time-steps. We also calculate the 'mean density' of each orbit, by calculating at each step the density of the model at the point visited by the orbit, and then taking the mean of these values. This 'mean density' is used to weight the orbit, as it can be considered as a first approximation for its importance. Thus the relative significance of the stable families for the dynamics of our model can be estimated by weighting the orbits by their 'mean density'. This is particularly important in regions where several families coexist. Using a program specifically made for this task and based on ESO-MIDAS routines, we construct an image (normalized over its total intensity) for each calculated and weighted orbit. The selected weighted orbits are then combined to build a profile. Darker parts of the profile image correspond either to regions occupied by a single family of relatively high importance, or to regions where many different orbits coexist.

To give a visual impression of the morphology supported by the different stable families we consider orbits from all families that could play a role. These are families having stable parts for large energy intervals. An exception are families born at the radial 3 : 1 resonance region, because as we have seen in Papers I and II their role for the dynamics of the studied models is only local. The selected orbits are equally spaced in their mean radius. This step in mean radius was the same for all families in a model. By over-plotting these orbits one gets a crude impression of the edge-on structure of a stellar model, constructed on the basis of the selected families. Such figures are not density maps like those presented in the 2D case in Contopoulos & Grosbøl (1988) and Patsis, Contopoulos & Grosbøl (1991), since we deal here only with periodic orbits. The diagrams should rather be considered as skeletons of supported structures.

The 3D families appear in pairs that are symmetric with respect to the $x = 0$, $y = 0$ and $z = 0$ planes. The (x, y) projections of the orbits of most families are identical to those of their symmetric pairs. That means that in most cases there is no morphological difference in the face-on view if we add the symmetric branches. On the other hand, in several cases, it is necessary to populate all symmetric branches to obtain symmetric edge-on profiles.

We present for all our models both the profiles of each family separately and also combined profiles, where we consider all or some of the families of the model. When we estimate the relative importance of periodic orbits for the building of the vertical profile in a galaxy, we have to take into account the fact that stable periodic orbits may reach large distances in the z-direction. This means that stable orbits with high $\overline{|z|}$ values are of lesser importance than the orbits remaining close to the equatorial plane and enhancing the bar. For the sake of completeness, however, we included these orbits in our profiles and we comment on their importance in each individual case.

3 PROFILES OF FAMILIES

In this section we present the edge-on profiles of the various families in each model. In the present paper we again use model A1 as a fiducial case. We describe the contribution of all its families to the profiles, while for the rest of the models we give mainly the differences of their orbital behaviour from what we find in model A1.

3.1 Model A1

Model A1, introduced in Paper I, includes a typical Ferrers bar, and has both a radial and a vertical 2 : 1 resonance. In Fig. 1 we give the side-on profiles of all important 3D families for this model that we found in Paper I. All panels are profiles of individual families. Throughout the paper we use a linear gray scale (i.e. a linear look-up-table in MIDAS) to display images.

Visually we can separate the profiles in two classes. Those for which the projections of their orbits pass through the projected centre of the system, i.e. the (0, 0) point, and those for which the (0, 0) point is at the centre of an empty region. To the first class belong the orbits of the families x1v4 (Fig. 1c) and x1v7 (Fig. 1e), the family of the 3D x2-like orbits of multiplicity 2 (Fig. 1g) and the 3D banana-like orbits of the family ban3v1 (Fig. 1h). Two of these families, x1v4 and x1v7, belong to the x1-tree. Their common characteristic is that they are bifurcations of x1 in $\dot{z}$, i.e. they have initial conditions $(x_0, \dot{x}_0, z_0, \dot{z}_0) = (a, 0, 0, b)$, with $a, b \in \mathrm{R}$ and $a, b \neq 0$, while $y_0 = 0$ and $\dot{y}_0 > 0$. We note that the structures they support are more '$\supset\subset$'-like than 'X'-like features. In that respect these families favour the presence of normal and not 'X'-shaped peanuts.

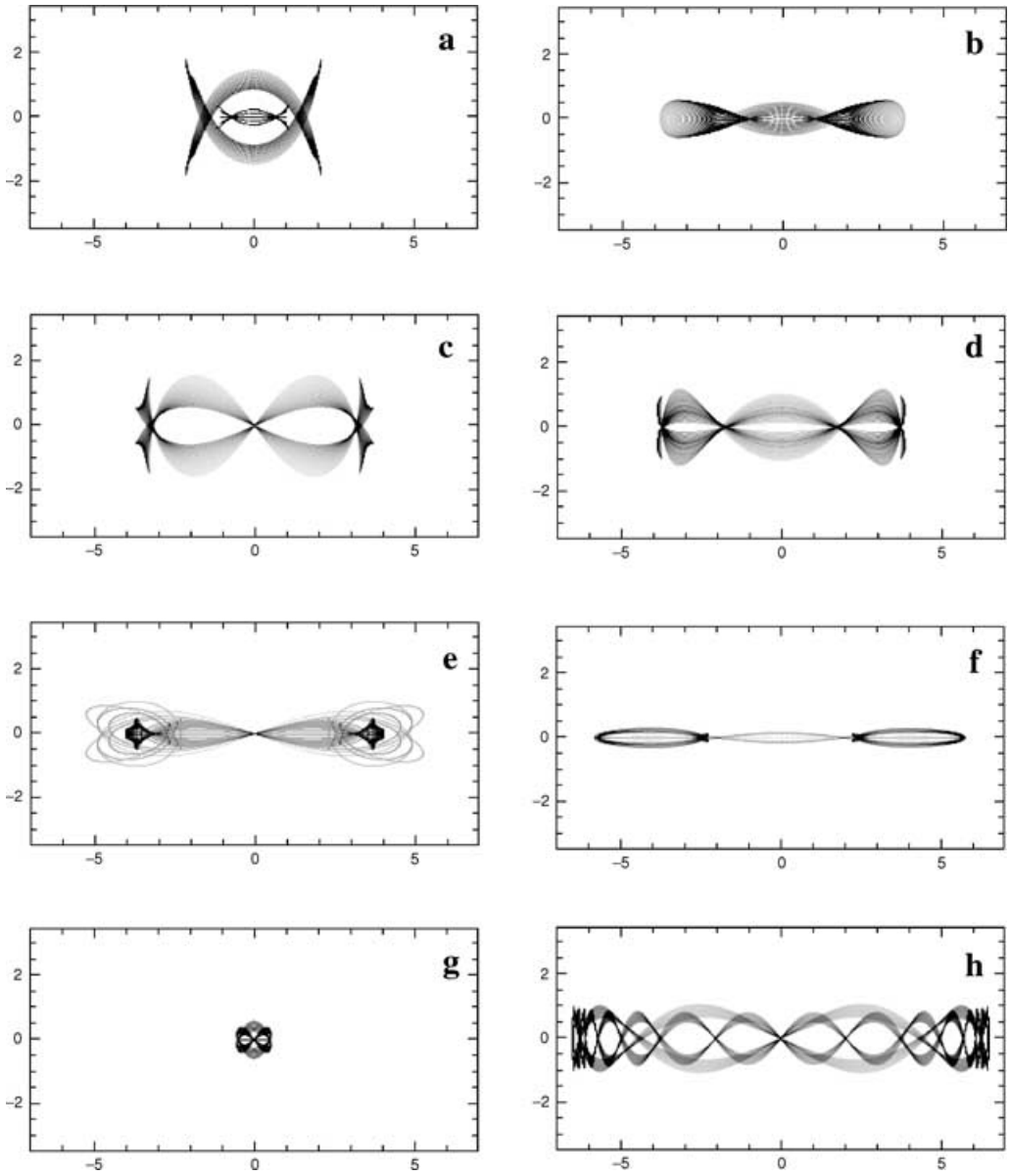

Figure 1. The profiles of the 3D families of model A1 viewed side-on. Each panel corresponds to one family: (a) x1v1, (b) x1v3, (c) x1v4, (d) x1v5, (e) x1v7, (f) x1v9, (g) x2mul2, and (h) ban3v1. In model A1 corotation is at 6.13. We use a different contrast in each figure in order to bring out best the morphology of the profile of each family.

The profiles that result from the superposition of stable orbits of the families x1v1 (Fig. 1a), x1v3 (Fig. 1b), x1v5 (Fig. 1d) and x1v9 (Fig. 1f), belong to the second class of profiles, which have an empty central region.

In order to quantify the morphologies supported in the various cases we use the $B_{\rm L}/O_{\rm Ly}$ ratio. Here $B_{\rm L}$ is the bar length and $O_{\rm Ly}$ is the orbital length of the family under consideration. $B_{\rm L}$ is estimated by considering the extent of all stable orbits *supporting* the bar. These are in general families of the x1-tree (Papers I and II). We project them on the semi-major axis, and the longest projection is $B_{\rm L}$. In some cases (see the case of x1v7 family below) we give in addition a second value for the $B_{\rm L}/O_{\rm Ly}$ ratio taking into account for the estimation of $B_{\rm L}$ also orbits of a family which do not fully support the bar (e.g. they have loops off the major axis, which extend in large distances). This number can be less than 1. We estimate $O_{\rm Ly}$, the orbital length, again by projecting orbits on the semi-major axis. However, for $O_{\rm Ly}$, we only take into account the orbits of the family we consider. The 'bar length' characterizes a model globally, while the 'orbital length' characterizes the (y, z) projection of a given family in the model. Because we investigate the contribution of the families to the boxy structures and to b/p features in general, these ratios should be compared with the corresponding ratios given by Lütticke et al. (2000b) for observations and Athanassoula & Misiriotis (2002) for *N*-body simulations. This will be done in Section 5.

In particular we can remark about the profiles of model A1 the following:

In general, the families which have at the centre an '$\supset\subset$' morphology are good candidates to build, or at least to support, the peanut feature. Family x1v4 (Fig. 1c) has an '∞'-type profile with two density enhancements added to its sides. Tangents to the inner parts of this '∞' feature passing through the centre have an angle to

the major axis of $\approx 22^\circ$. The empty inner parts of the '∞' feature reflect the fact that this family is born as unstable and thus lacks members lying almost on the equatorial plane, i.e. with low $\overline{|z|}$. The 'bar length', in model A1 reaches $r \approx 4.5$ (Patsis, Skokos & Athanassoula, 2002b; hereafter Paper IV) thus for the family x1v4 we have $B_L/O_{Ly} \approx 1.3$.

x1v7 (Fig. 1e) also clearly harbours an '$\supset\subset$' feature. The angle to the major axis now is $\approx 12^\circ$. A box is vaguely defined, but now it is thin since the orbits remain close to the equatorial plane. The profile is better described as having a '∞' morphology with a low $\overline{|z|}$ and with two characteristic local enhancements of the surface density at $|y| \approx 3.8$ along the major axis. The B_L/O_{Ly} ratio is ≈ 1.2 if we consider as edges the enhancements, or ≈ 0.9 if we include the few outermost orbits as well. These outermost orbits are 4 : 1 rectangular-like orbits with loops at their four apocentra in their (x, y) projections. Their contribution to the density of the bar and to its face-on morphology is discussed in Paper IV. Nevertheless these outermost orbits are not considered as contributing to the extent of the bar towards corotation.

Note that both x1v4 and x1v7 have local enhancements along the major axis, which are symmetric with respect to the centre and are manifestations of the orbital character of the profile. If the edge-on profile of a galaxy is determined by families like x1v4 and x1v7, then both the '$\supset\subset$' morphology and the local enhancements on the major axis should be observed (see Section 5 below).

The peanut that could be supported by the x2mul2 family is confined to the central region of the disc (Fig. 1g). This is expected because the projections of the orbits of this family on the equatorial plane are oriented along the minor axis of the main bar. For this family we have $B_L/O_{Ly} \approx 9$. x2mul2 could be useful to explain structures embedded in the very centres of edge-on disc galaxies.

Finally the ban3v1 3D banana-like orbits favour in this projection the presence of an '$\supset\subset$' structure in the central region of a model.

Side-on profiles with empty regions around the central point (0, 0) are provided by the families x1v1 and x1v5, both proposed in the past as peanut-building families (Combes et al. 1990; Pfenniger & Friedli 1991; Pfenniger 1984a, 1985). The x1v1 profile (Fig. 1a) consists of two parts, an inner and an outer one. This reflects the fact that the evolution of the stability of family x1v1 follows a S $\rightarrow \Delta \rightarrow$ S transition (Paper I) and thus its stable parts exist for two separated energy intervals. The gap is formed because only stable orbits should be considered. Actually the missing complex unstable part of the family would have provided very useful members for building the boxy bulge, in the sense that this family now provides only orbits with either very low or with relatively high $\overline{|z|}$. The outer part has 'wings' at the left- and right-hand sides, which could bring in the system pieces of an 'X' structure. These pieces, however, do not continue towards the centre. The central area separates the two pieces of the 'X'. We will refer to this kind of morphology with the symbol '$\bowtie$'. We note that the wings reach from the equatorial plane to their maximum height very abruptly over a distance $\Delta y \approx 0.4$ and that the successive weighted orbits overplotted form four sharp peaks. The 'orbital length' reaches a distance from the centre $r \approx 2.1$, so the B_L/O_{Ly} ratio for family x1v1 is about 2.1. If the outer part of the family, after the S $\rightarrow \Delta$ transition, is not populated, then we have $B_L/O_{Ly} \approx 4.1$. In this case, however, we would have orbits confined close to the centre with small deviations from the equatorial plane. Velocity dispersion will smooth out such features and due to dust they will not be easily observed in edge-on real galaxies.

Families x1v3 and x1v5, although bifurcated at different vertical resonances, can give similar side-on profiles (cf. Figs 1b and d). This is a good example to show that it is the superpositions of stable orbits of a family, i.e. the vertical profile in a model, and not just the morphology of single orbital representatives, that can decide about the supported morphologies. Since the 'bar length' in model A1 is $\approx$4.5, both families have $B_L/O_{Ly} \approx 1.2$.

Family x1v9 remains always close to the equatorial plane. It does not directly support the bar, as its (x, y) projection consists of 4 : 1 rectangular like orbits with big loops. Furthermore, it does not contribute much to specific features, like boxes, observed in vertical profiles. Because it is not considered as a family helping the bar to come closer to corotation, we do not give in this case orbital ratios.

A common feature encountered in all four families in model A1 with a '$\bowtie$' vertical morphology is that, independent of the vertical resonance at which they are bifurcated, their side-on profiles are characterized by three local maxima above the equatorial plane. This is a disadvantage for using them for building peanuts, as b/p bulges have two such local maxima. These families could nevertheless give to the model an overall boxy side-on morphology, but only if we consider orbits trapped around the periodic ones. This can be achieved more easily with the x1v1 family because its orbits reach higher $\overline{|z|}$ distances.

In Fig. 2 we give the end-on, (x, z), profiles for the 3D families in model A1, i.e. we change our viewing angle by 90° and view along the bar major axis. Comparing Figs 1 and 2 we note that in several cases the side-on and the end-on views of the same family have different central morphology. The families x1v3 and x1v4 are typical examples, as the (x, z) morphology of one is similar to the (y, z) morphology of the other. As in the side-on views their profiles belong to different classes, the same holds for their end-on views, but now x1v3 has a '$\supset\subset$' and x1v4 a '$\bowtie$' central morphology, i.e. opposite to their side-on projections. The same happens to the profiles of x1v7 (cf. Fig. 1e with Fig. 2e), x2mul2 and the banana-like 3D orbits of family ban3v1. Thus x1v3 is the only family with an '$\supset\subset$' type end-on morphology. Viewing a barred galaxy end-on, it does not make sense to compare the extent of the (x, z) projection of a family with the length of the bar, since the feature we study is *across* the bar. Therefore, we will use the ratio of the corotation radius over the (x, z) orbital length (R_{cor}/O_{Lx}) of the family in order to assess its relative length and its extent on the galactic disc. 'R_{cor}' indicates the corotation radius, which in model A1 is 6.13, and 'O_{Lx}' is the orbital length derived from the projection of the family on the minor axis (similarly to the definition of 'O_{Ly}' for the projection on the major axis). Another general remark is that the (x, z) projections of the profiles are in most cases smaller than their (y, z) projections. This is particularly true for the families which are introduced in the system at low energies, i.e. x1v1, x1v3 and x1v4 shown in Figs 2(a), (b) and (c) respectively. Especially for x1v1, if we consider only the part of the family before the S $\rightarrow \Delta$ transition, then its end-on profile is tiny and thus the R_{cor}/O_{Lx} ratio becomes huge. The rest of the 3D families bifurcated from x1 have comparable 'orbital lengths' in both projections. However, we have to note that families of the x1-tree that are bifurcated closer to corotation remain confined close to the equatorial plane and thus are less likely to characterize the morphology of the b/p structure.

In particular, for the (x, z) profiles of each family we can say the following:

The x1v3 (x, z) projection (Fig. 2b) now harbours an '$\supset\subset$' feature embedded in a boxy feature with $R_{cor}/O_{Lx} \approx 4.7$. All other profiles are of an '$\bowtie$'-type morphology. The x1v1 family (Fig. 2a) has $R_{cor}/O_{Lx} \approx 6.8$. The end-on projection of the orbits of this family reveals a bulge-like component with pieces of an 'X' feature located closer to the centre than in the corresponding (y, z)

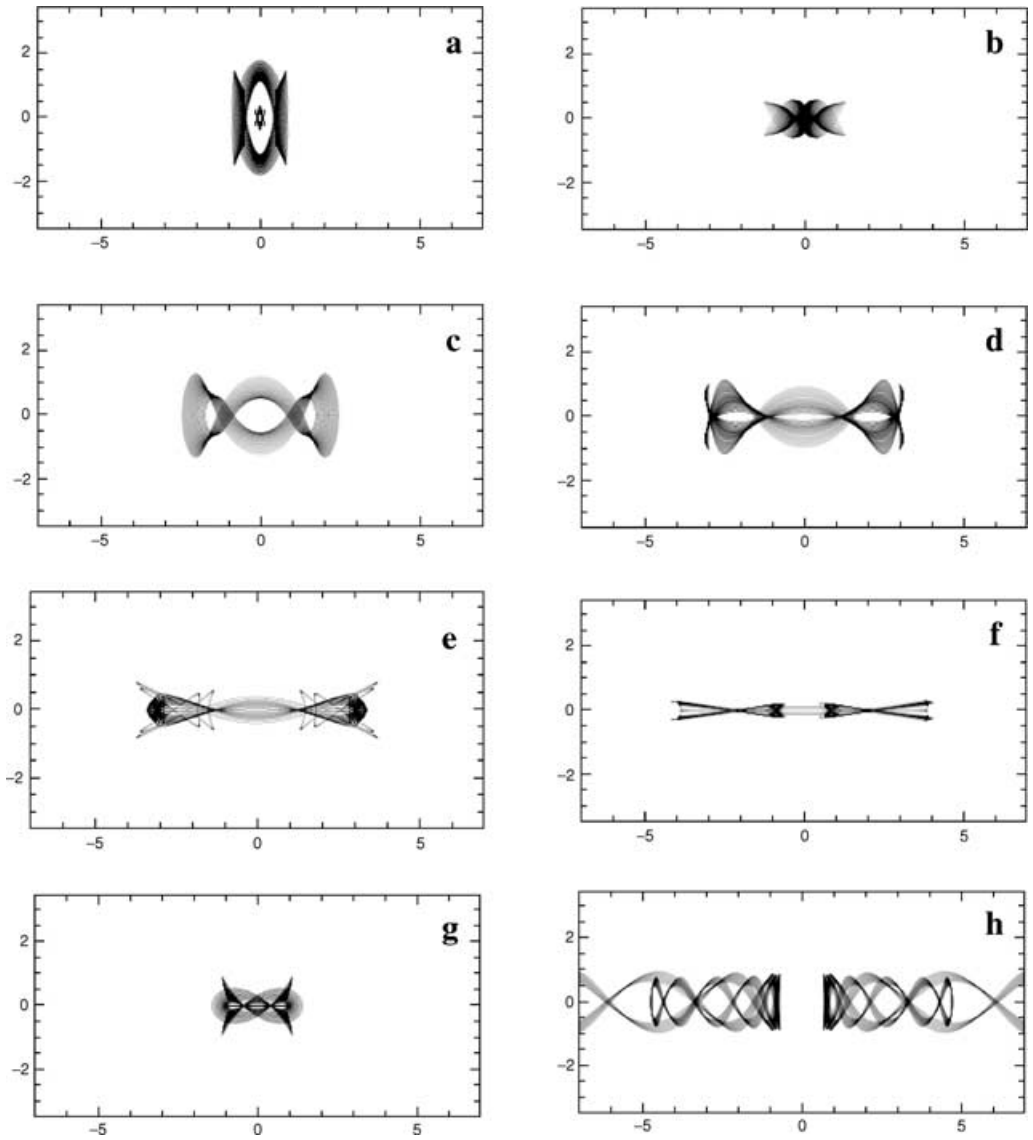

Figure 2. The profiles of the 3D families of model A1 viewed end-on. The layout is as in Fig. 1.

projection. Again, one sees that the most useful orbits of this family for building an 'X' are missing because they are complex unstable. It is also evident that the end-on view of this family supports a morphology that is more extended in the z- than in the x-direction, if the outer part of the family is populated. Such a feature is not observed in edge-on disc galaxies. That means that either such features are smoothed out by dispersion, or that they are embedded in larger and rounder bulge components, or that the x1v1 orbits beyond the first S $\rightarrow$ Δ transition are not populated.

The (x, z) projection of x1v4 (Fig. 2c) has three local maxima, and has $R_{\rm cor}/O_{\rm Lx} \approx 2.5$, i.e. it is quite extended along the equatorial plane. This reflects the fact that many stable orbits of x1v4 in their (x, y) projections are close to hexagons with roughly equal extensions along the x and y directions (see Paper I). The same holds also for the family x1v7 (Fig. 2e), which has $R_{\rm cor}/O_{\rm Lx} \approx 1.8$ and whose orbits are quite rectangular in their face-on projection. The (x, z) projection of x1v7 has a third local maximum, which, however, is very close to the equatorial plane. In this projection the x2mul2 family supports a small peanut with $R_{\rm cor}/O_{\rm Lx} \approx 4.4$. The profile of family x1v9 (Fig. 2f) is very thin in this projection as well. Finally the 3D banana-like orbits of family ban3v1 (Fig. 2h) can contribute to the boxiness of a central structure, by enhancing the sides of a box at radii less than 1 kpc, even if the central area remains empty.

To some degree, the presence of the third central local maximum seen in the profiles in Figs 1 and 2 depends on the viewing angle, always considered to be on the equatorial plane. In the above we considered only the side-on and end-on views, but intermediate viewing angles can be considered in the same way. In most of the cases we examined there is a range of projection angles where the overlapping of orbits of a family can be responsible for the morphology of a continuous '⊃⊂' feature inside a box. In other words, by changing the viewing angle we can minimize the importance of the third local maximum in z, which is not consistent with a peanut morphology, and at the same time bring the two separated pieces of an 'X' closer. However, one should not overestimate the role of rotation, because the range of viewing angles that reproduce the 'X' morphology is narrow. In the case of the x1v1 family of model A1,

Table 1. Properties of edge-on profiles in model A1. At the top row we summarize the properties of the model. G is the gravitational constant, M_D, M_B, M_S are the masses of the disc, the bar and the bulge respectively, ϵ_s is the scale length of the bulge, Ω_b is the pattern speed of the bar, E_j (r-IILR) is the Jacobian for the inner radial ILR, E_j (v-ILR) is the Jacobian for the vertical 2 : 1 resonance, R_c is the corotation radius, and $B_{\rm L}$ is the longest projection of bar supporting orbits on the semi-major axis. The comment characterizes briefly the model. The successive columns of the main table give the name of the family, the vector of the initial conditions on the Poincaré surface of section defined by $y_0 = 0$ and $\dot{y_0} > 0$, essentially describing if we have a vertical bifurcation of x1 in z or $\dot{z}$, the $B_{\rm L}/O_{\rm Ly}$ ratio, a symbol indicating the central morphology supported by the orbit in the side-on view (s/o), the $R_{\rm cor}/O_{\rm Lx}$ ratio, a symbol indicating the central morphology supported by the orbit in the end-on view (e/o), and finally a comment about special features of the particular profile.

Model name	GM_D	GM_B	GM_S	ϵ_s	Ω_b	E_j (r-IILR)	E_j (v-ILR)	R_c	$B_{\rm L}$	Comments
A1	0.82	0.1	0.08	0.4	0.0540	−0.441	−0.360	6.13	4.5	Fiducial

Family	Initial conditions	$B_{\rm L}/O_{\rm Ly}$	s/o shape	$R_{\rm cor}/O_{\rm Lx}$	e/o shape	Comments
x1v1	$(x, z, 0, 0)$	4.1/2.1	⋈	41/6.8	⋈	Two stable parts (see text)
x1v3	$(x, z, 0, 0)$	1.2	⋈	4.7	⋋⋌	
x1v4	$(x, 0, 0, \dot{z})$	1.3	⋋⋌	2.5	⋈	
x1v5	$(x, z, 0, 0)$	1.2	⋈	2.0	⋈	
x1v7	$(x, 0, 0, \dot{z})$	1.2/0.9	⋋⋌	1.8/1.7	⋈	Partly not bar-supporting
x1v9	$(x, z, 0, 0)$	–	⋈	1.5	⋈	Not bar-supporting
x2mul2	$(x, z, 0, 0)$	9	⋋⋌	4.4	⋈	Along the minor axis of the bar
ban3v1	$(x, 0, 0, \dot{z})$	–	⋋⋌	–	][	Not bar-supporting

a 'X' feature due to rotation is discernible only in an angle range $\Delta\theta \leqq 15^\circ$ close to the (x, z)-projection.

In Table 1 we summarize the properties of the edge-on orbital profiles in model A1. The symbols used for describing the central morphologies are explained in the text, except for '][' used for the central end-on morphology of the 3D banana-like orbits of the family ban3v1. The two branches of this family appear at the sides of the bar, symmetric with respect to its major axis, and leave a totally empty region at the centre of the end-on profile.

3.2 Model A2

Model A2 differs from A1 only in the pattern speed (Paper II), which is so much slower that its inner Lindblad resonance that it is roughly at the radius where model A1 has its corotation.

In Fig. 3 we give the (y, z) projections of the four families that can essentially affect the appearance of the vertical profile of the model. It is evident that in this projection b/p bulges can be associated with either of the families x2v1 (Fig. 3a) and x1v1 (Fig. 3b). The other two families have profiles that remain close to the equatorial plane while reaching in this plane close to corotation and thus can be associated only with the vertical structure in the outer parts of the bar. This is even more the case for the rest of the stable 3D families of model A2 described in Paper II (x1′v4, x1′v5), as they remain very close to the equatorial plane and do not influence the edge-on morphology of the model. The projection of the bar-supporting orbits in model A2 on the semi-major axis reaches a distance from the centre $r \approx 9.4$. So we have $B_{\rm L}/O_{\rm Ly} \approx 2.1$ for the x1v1 family and $B_{\rm L}/O_{\rm Ly} \approx 4.7$ for x2v1 (the x2v1 orbits are elongated along the minor axis of the main bar). The superposition of x1v1 orbits will give to the system a very sharp and continuous 'X' feature despite the fact that individual orbits do not support this morphology, even if we take into account both branches which are symmetric with respect to the equatorial plane. The reason for this is that the gap due to the complex unstable part at the S → Δ → S transition is negligible. Family x2v1 has a '⋈' feature in the centre.

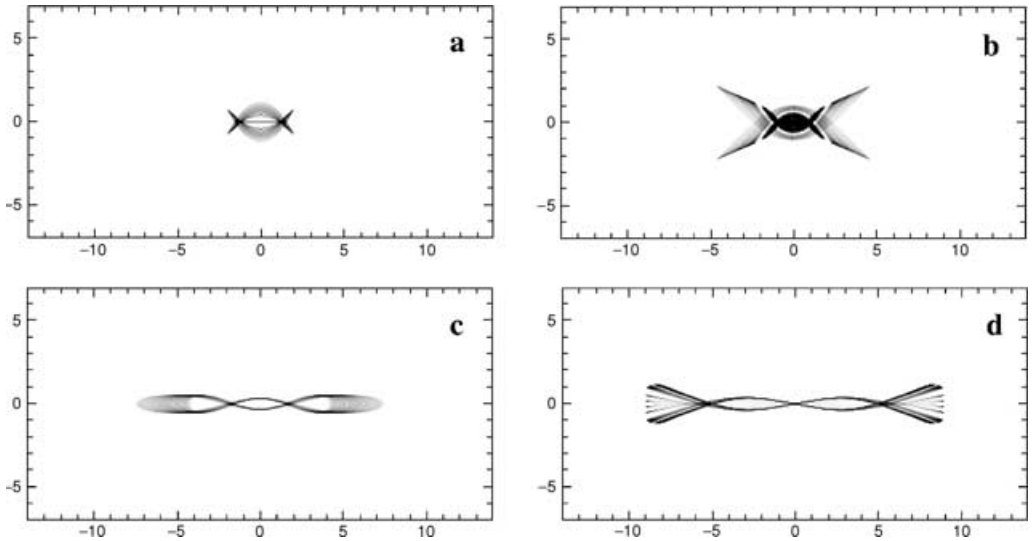

Figure 3. The side-on profiles of the main relevant families of model A2. Each panel corresponds to another family: (a) x2v1, (b) x1v1, (c) x1v3 and (d) x1v4. In model A2 corotation is at 13.24.

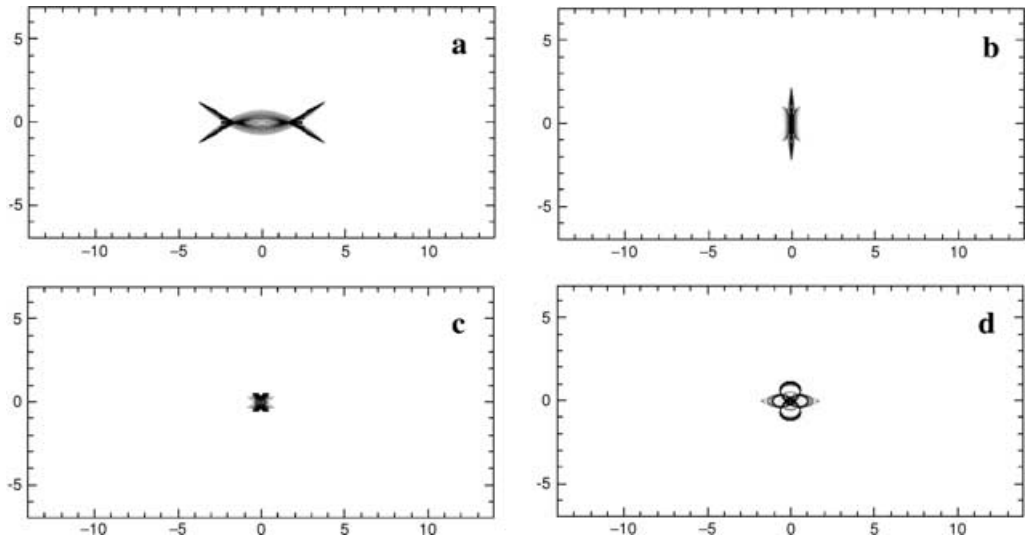

Figure 4. The end-on profiles of the main relevant families of model A2. The layout is as in Fig. 3.

If we rotate the model by $\pi/2$ the families will give the projected profiles depicted in Fig. 4. In this projection also it has a '⋈' central part (Fig. 4a) and remains relatively close to the equatorial plane. The x1v1 profile in this projection almost vanishes squeezed on the rotational axis (Fig. 4b). The x1v3 profile can be described as a tiny 'x', while that of x1v4 can be described as a quadrupole feature made of the overlapping of an '8' and an '∞' symbol. We remind the reader here that in all these profiles we consider both, symmetric with respect to the equatorial plane, branches of each family. If due to the presence of a an external factor (e.g. a companion) only one branch is populated then the above symmetry will break, and instead of e.g a tiny 'x' feature, in the case of x1v3, this family will support the presence of a tiny '∼' feature.

The properties of the profile of each family are summarized in Table 2. Topologically, the central morphology of a family is of course similar in all models. However, in the tables we prefer to refer to symbols that characterize the specific morphology in each case. Therefore we describe in model A2 (Table 2) the central side-on x1v1 morphology with the symbol 'X', while to the end-on central morphologies of the families x1v1, x1v3 and x1v4 we attribute the symbols '|', 'X' and '8/∞', respectively.

3.3 Model A3

Model A3 is the same as model A1, except that its bar is rotating faster (Paper II). The main 3D families which could build its vertical structure are x1v1, x1v3, x1v5, x1v8 and q0v1, the 3D bifurcation of family q0 (Paper II). Their (y, z) profiles are given in Fig. 5.

At the side-on projections only q0v1 has at the centre a '⊃⊂' morphology. However, this is again a 4 : 1 radial resonance family whose orbits have four big loops and thus does not directly support the bar. Also its range of existence is narrow. All other profiles have a central region that can be described with the symbol '⋈'.

As we see in Fig. 5(a) the x1v1 profile is characterized by a large empty part because of the complex unstable region. In the stable part beyond the $\Delta \rightarrow$ S transition the family only gives proportionally few orbits in relatively low heights above the equatorial plane. For energies somewhat larger than the energy of the outermost x1v1 orbit plotted in Fig. 5(a), the orbits reach vertical distances with $|z| = 2$, turning simultaneously towards lower $|y|$ values; they are not given in Fig. 5(a). The rest of the side-on profiles do not have essential differences from what we encountered in the fiducial model.

Contrary to the side-on, the end-on projections (Fig. 6) of the families x1v3 (Fig. 6b) and x1v5 (Fig. 6c) support the presence of b/p features. The x1v5 profile is characterized in addition by two local enhancements of the surface density along the minor axis which are symmetric with respect to the centre. The size of these b/p structures is small compared to the corotation radius and gives $R_{\rm cor}/O_{\rm Lx} = 3.5$ both for the x1v3, and for the x1v5 family. x1v8 (Fig. 6d) and especially q0v1 (Fig. 6e) are less important for the end-on vertical structure of the model. All of the families, except for x1v1 which anyway vanishes in the end-on projection (Fig. 6a), give profiles with a '⊃⊂' central morphology. In conclusion, model A3 can give only confined boxy profiles when viewed end-on.

The properties of the profile of each family are summarized in Table 3. The two ratios given in Table 3 in the $B_{\rm L}/O_{\rm Ly}$, as well as in the $R_{\rm cor}/O_{\rm Lx}$, columns, refer to the x1v1 orbits as plotted in Figs 5(a) and 6(a). By adding a question mark in a parenthesis after

Table 2. Properties of edge-on profiles in model A2. The columns are as in Table 1.

Model name	GM_D	GM_B	GM_S	ϵ_s	Ω_b	E_j (r-IILR)	E_j (v-ILR)	R_c	$B_{\rm L}$	Comments
A2	0.82	0.1	0.08	0.4	0.0200	−0.470	−0.357	13.24	9.4	Slow bar

Family	Initial conditions	$B_{\rm L}/O_{\rm Ly}$	s/o shape	$R_{\rm cor}/O_{\rm Lx}$	e/o shape	Comments
x2v1	$(x, z, 0, 0)$	4.7	⋈	3.6	⋈	Along the minor axis of the bar
x1v1	$(x, z, 0, 0)$	2.1	X	26.5	|	
x1v3	$(x, z, 0, 0)$	1.3	⋈	16.6	×	
x1v4	$(x, 0, 0, \dot{z})$	1.1	⋈	7.8	8 and ∞	

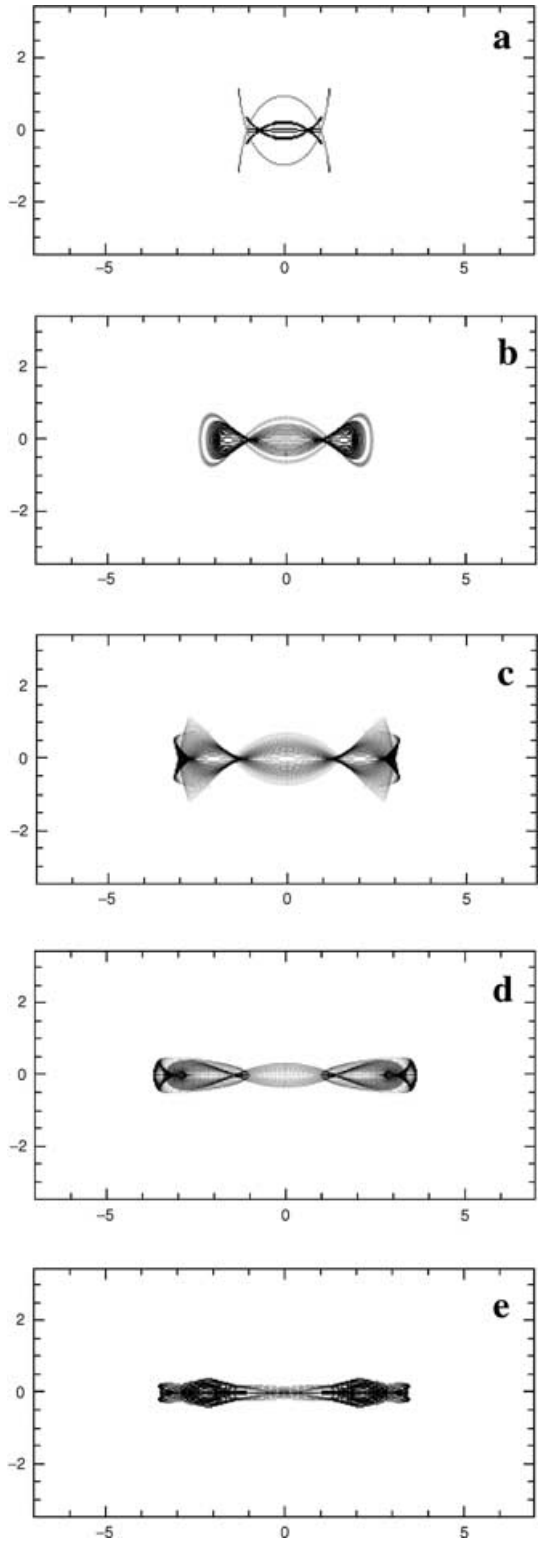

Figure 5. The side-on profiles of the families of model A3. Each panel corresponds to another family: (a) x1v1, (b) x1v3, (c) x1v5, (d) x1v8 and (e) the 3D bifurcation of q0, i.e. q0v1. In model A3 corotation is at 4.19.

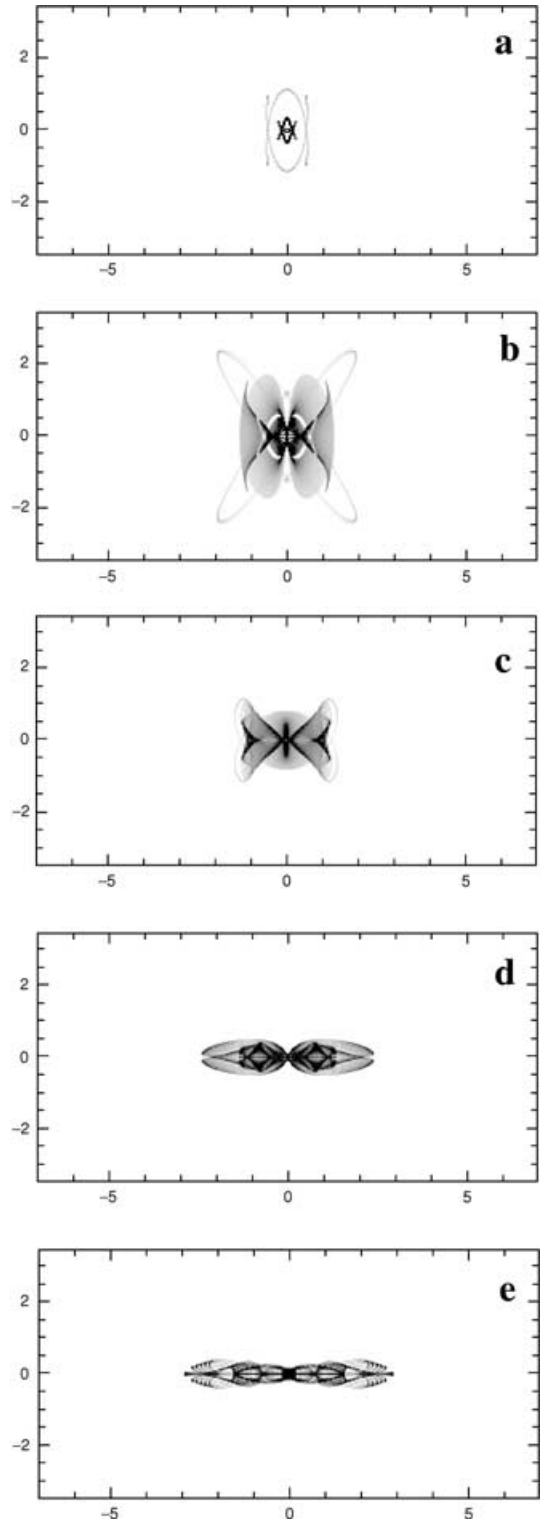

Figure 6. The end-on profiles of the families of model A3. The layout is as in Fig. 5.

the symbol 'X', which characterizes the central end-on morphology of the family x1v5, we want to underline that, although the family supports the 'X' morphology, the confined extent of its end-on projection will apparently lead just to a boxy profile.

3.4 Model B

As described in Paper II, model B has the same total mass as the fiducial one but lacks an explicit bulge component. It has neither radial, nor vertical 2 : 1 resonances, and its bar rotates as fast as that of model A1. As there are no x1v1 orbits close to the centre to

Table 3. Properties of edge-on profiles in model A3. The columns are as in Table 1.

Model name	GM_D	GM_B	GM_S	ϵ_s	Ω_b	E_j (r-IILR)	E_j (v-ILR)	R_c	B_L	Comments
A3	0.82	0.1	0.08	0.4	0.0837	−0.390	−0.364	4.19	3.8	Fast bar

Family	Initial conditions	B_L/O_{Ly}	s/o shape	R_{cor}/O_{Lx}	e/o shape	Comments
x1v1	$(x, z, 0, 0)$	3.8/3.2	⟩⟨	16.8/7.0	⟩⟨	
x1v3	$(x, z, 0, 0)$	1.6	⟩⟨	3.5	⊃⊂	
x1v5	$(x, z, 0, 0)$	1.2	⟩⟨	3.5	X(?)	
x1v8	$(x, z, 0, 0)$	1.0	⟩⟨	1.7	⊃⊂	
q0v1	$(x, z, \dot{x}, \dot{z})$	1.1	⊃⊂	1.4	⊃⊂	Not directly bifurcated from x1

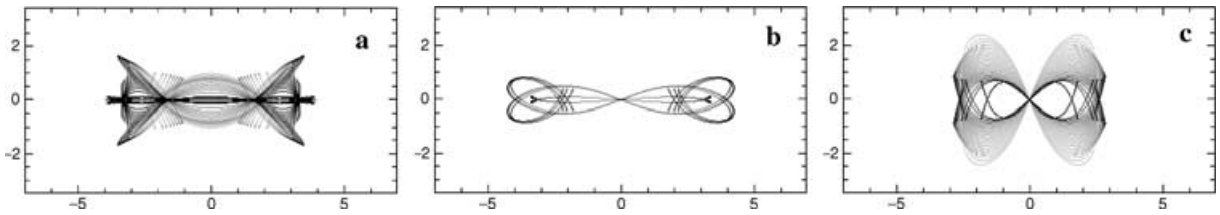

Figure 7. The side-on profiles of the families of model B. Each panel corresponds to another family: (a) x1v5 and x1v5′, (b) x1v7, (c) z3.1s. Model B has neither radial nor vertical 2 : 1 resonances and its corotation is at 6.

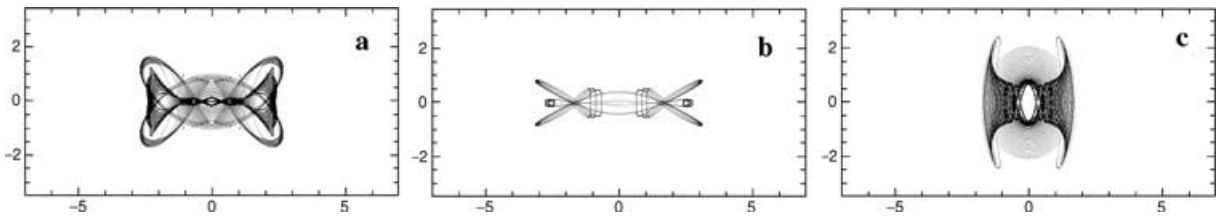

Figure 8. The end-on profiles of the families of model B. The layout is as in Fig. 7.

populate a boxy structure, and there is no Plummer sphere to influence the central dynamics of the model, one could have expected to have more flat edge-on profiles. This, however, is not the case, as we see in Fig. 7 for the profiles along the major axis and Fig. 8 for the profiles along the minor axis of the bar.

The families that could be related with boxy vertical structures in this model are the two families related to the vertical 4 : 1 resonance (x1v5, x1v5′), x1v7, and z3.1s. As we have seen in Paper II, the vertical bifurcations of x1 that give 3D orbits are x1v5, x1v5′, and x1v7; x1v5 being the first vertical x1 bifurcation in this model. Their side-on profiles give the boxy structures, which are depicted in Fig. 7(a) for x1v5 and x1v5′ together ($B_L/O_{Ly} \approx 1.1$), and Fig. 7(b) for x1v7 ($B_L/O_{Ly} \approx 1$). The outer orbits of x1v7, however, as in the fiducial case, are characterized in their face-on projection by an extreme 'butterfly' morphology *surrounding* all other orbits that support the bar. Furthermore, the inner orbits remain very close to the equatorial plane. Thus the significance of this and of other similar families is small. x1v5′ orbits also have at their largest energies a 'butterfly' morphology as well. Their (x, y) projections, however, are surrounded by the usual rectangular orbits at the 4 : 1 region (Paper IV). Also we note that, although the combined side-on profile of the two vertical 4 : 1 resonance families has three local maxima above the equatorial plane, as does x1v5 in model A1 (Fig. 1d), the central local maximum in model B is clearly lower than those on the sides, and this leads to a b/p morphology similar to that observed in edge-on galaxies with b/p profiles. Most interesting in this model is the side-on profile of the z3.1s family (Fig. 7c). As we have seen in Paper II, this family is not part of the x1 forest. It is connected to the z-axis orbits described three times. Fig. 7(c) shows that its profile supports a boxy structure, as well as the presence of a central '⊃⊂' morphology and thus makes a perfect peanut. The peanut has $B_L/O_{Ly} \approx 1.4$, while if we consider only the orbits that make the strong part of the '⊃⊂' we have $B_L/O_{Ly} \approx 2$.

The profiles along the minor axis can also be boxy (Fig. 8). x1v5 and x1v5′ build a well-defined peanut along the *minor* axis with $R_{cor}/O_{Lx} \approx 2.3$. The z3.1s profile could give either a boxy or a rounder bulge-like feature, depending on the degree of participation of the orbits with the largest energies, which give the horn-like morphology of this profile. If we include the high energy orbits, the profile has the form of a roundish bulge-like feature, slightly elongated along the rotational axis.

The end-on profile of family x1v7 is confined close to the equatorial plane (Fig. 8b), with a R_{cor}/O_{Lx} ratio about 1.9. Thus, in the presence of the orbits of the two other families it does not characterize the morphology of the central area of the model even in this projection.

The properties of the profile of each family of model B are summarized in Table 4.

3.5 Model C

Model C has a vertical, but no radial, 2 : 1 resonance. The edge-on and end-on profiles in this model are in general similar to those encountered in model A1. There is, however, a notable exception and this refers to the family x1v1, bifurcated at the vertical 2 : 1 resonance. x1v1, in this particular model, has an S → Δ transition

Table 4. Properties of edge-on profiles in model B. The columns are as in Table 1.

Model name	GM_D	GM_B	GM_S	ϵ_s	Ω_b	E_j (r-IILR)	E_j (v-ILR)	R_c	B_L	Comments
B	0.90	0.1	0.00	–	0.0540	–	–	6.00	3.9	No bulge

Family	Initial conditions	B_L/O_{Ly}	s/o shape	R_{cor}/O_{Lx}	e/o shape	Comments
x1v5/x1v5′	$(x, z, 0, 0)$	1.1	⟜⟝	2.3	⟜⟝	
x1v7	$(x, 0, 0, \dot{z})$	1	⟝⟜	1.9	⟜⟝	
z3.1s	$(x, 0, 0, \dot{z})$	1.4/2.0	⟝⟜	3.5	⟜⟝	Not part of the x1-tree

Table 5. Properties of edge-on profiles in model C. The columns are as in Table 1.

Model name	GM_D	GM_B	GM_S	ϵ_s	Ω_b	E_j (r-IILR)	E_j (v-ILR)	R_c	B_L	Comments
C	0.82	0.1	0.08	1.0	0.0540	–	−0.364	6.12	4.2	Extended bulge

Family	Initial conditions	B_L/O_{Ly}	s/o shape	R_{cor}/O_{Lx}	e/o shape	Comments
x1v1	$(x, z, 0, 0)$	2.3	X	6.8	⟜⟝	

at large energies (Paper II). It thus remains practically always stable and its orbits which do not reach large distances over the equatorial plane, could populate a boxy feature. Comparison of model C with model A1 demonstrates the role of the complex instability in the b/p profiles made by x1v1 orbits. In the present case the 'X' feature is not interrupted. This difference will become apparent in Section 5, where we compare the various morphologies of the models. The properties of the model and of the x1v1 family are summarized in Table 5.

3.6 Model D

A strong bar case is described in model D. The mass of the bar in model A1 is doubled at the expense of the disc mass, so that the total mass of the system is kept constant. Again we have collected the side-on and end-on profiles of the families in two figures; Fig. 9 for the (y, z) and Fig. 10 for the (x, z) profile. In this case we have, as in model B, two families associated with the vertical 4 : 1 resonance (Paper II).

In the side-on views families x1v1, x1v3, x1v5 and x1v5′ have central regions characterized by an '⟜⟝' feature. In Fig. 9(a) we observe that the main part of the profile consists of x1v1 orbits which are nested one inside the other, in such a way as to build outside of the central empty region parts of the four sides of an 'X' feature. The difference with the corresponding profile of the fiducial case (Fig. 1a) is that the branches of the 'X' are now more extended. In Fig. 1(a) the pieces of the 'X' branches emerging out of the empty region reach $|z| \approx 1.5$ in a distance of $\Delta y \approx 0.5$, while in Fig. 9(a) in a distance of $\Delta y \approx 1$. In model D, the family x1v1 undergoes a S $\rightarrow$ Δ $\rightarrow$ S transition, like in model A1. Model D, however, is more suitable than model A1 to describe b/p features because in this model the orbits needed for building the peanut are stable and not complex unstable. As the bar is more massive, the potential well is deeper than that of model A1. Thus the family x1v1 is bifurcated at a smaller energy than in model A1, becomes complex unstable, and when it turns again stable the orbits have relatively low $\overline{|z|}$. The ratio B_L/O_{Ly} is ≈2.4. A secondary gap in the succession of the x1v1 orbits that can be seen in Fig. 9(a), is due to a small instability strip (Fig. 16 in Paper II) at which x1v1 has a simple unstable part. This gap, however, is bridged by a stable bifurcation of x1v1, called x1v1.1. The x1v3 orbits (Fig. 9b) reach lower $|z|$ values than those of x1v1. They could affect the vertical profile, but not in the central region. Finally, we have the two families bifurcated at the vertical 4 : 1 resonance area: x1v5 with elliptical-like orbits with loops along the major axis at their face-on projections and x1v5′ with rectangular like orbits in the (x, y) projection. In the side-on profile the x1v5 orbits remain close to the equatorial plane, while the orbits of x1v5′ reach large $|z|$. In both cases the contribution of the family is not important for the vertical structure of this model because of the mean deviation of the orbits from the equatorial plane. The families x1v6 and x1v7 have in the central regions of their side-on profiles a '⟝⟜' feature. In this model x1v6 has some stable representatives, but they remain always close to the $z = 0$ plane and its B_L/O_{Ly} ratio is close to 1. x1v7 gives a b/p vertical structure with a ratio $B_L/O_{Ly} \approx 1.2$. This means that most of the bar participates in the b/p morphology.

Viewed end-on, the x1v1 profile gives a bulge-like feature, rather elongated along the z axis of rotation. x1v7, although it shows in this projection the three z maxima morphology, can be described as boxy or peanut-shaped, because the two clumps at the sides are much denser than the middle one. Finally, in this projection, family x1v3 could provide a confined boxy feature.

The properties of the model and of the profiles are summarized in Table 6. In effect, in the box of the side-on morphology of x1v1, which is essentially of '⟜⟝' type, we can see segments of a 'X' feature. Segments of 'X' can also be seen in the boxy end-on profile of the family x1v3. However due to its large R_{cor}/O_{Lx} ratio, the addition of dispersion in the velocities of the orbits will result in a boxy feature. These peculiarities are indicated by the symbols we use in Table 6.

4 COMPOSITE PROFILES

So far we presented separately the building blocks that each family provides to the vertical structure of a model. However, the vertical structure of a real galaxy could be specified by more than one family. So we created composite profiles as well, taking into account all, or some, of the families of the model in each case. In this kind of representations the images of the profiles we have seen until now are added together to give a single image.

In Fig. 11(a), we consider all families of model A1 presented in Fig. 1, except for the banana-like orbits. If we select just the families x1v4, x1v7 and x1v9 we obtain the profile we see in Fig. 11(b). In principle there is no reason to include in a system all families

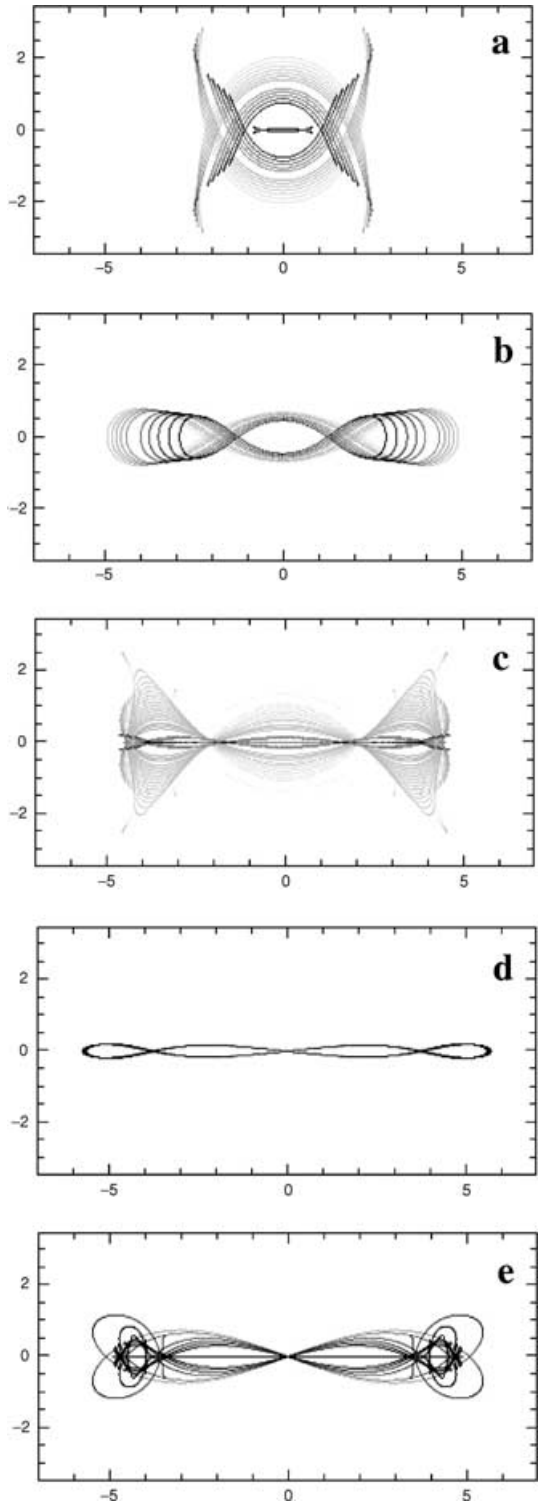

Figure 9. The side-on profiles of the families of model D. Each panel corresponds to another family: (a) x1v1, (b) x1v3, (c) x1v5 and x1v5′, (d) x1v6, (e) x1v7. In model D corotation is at 6.31.

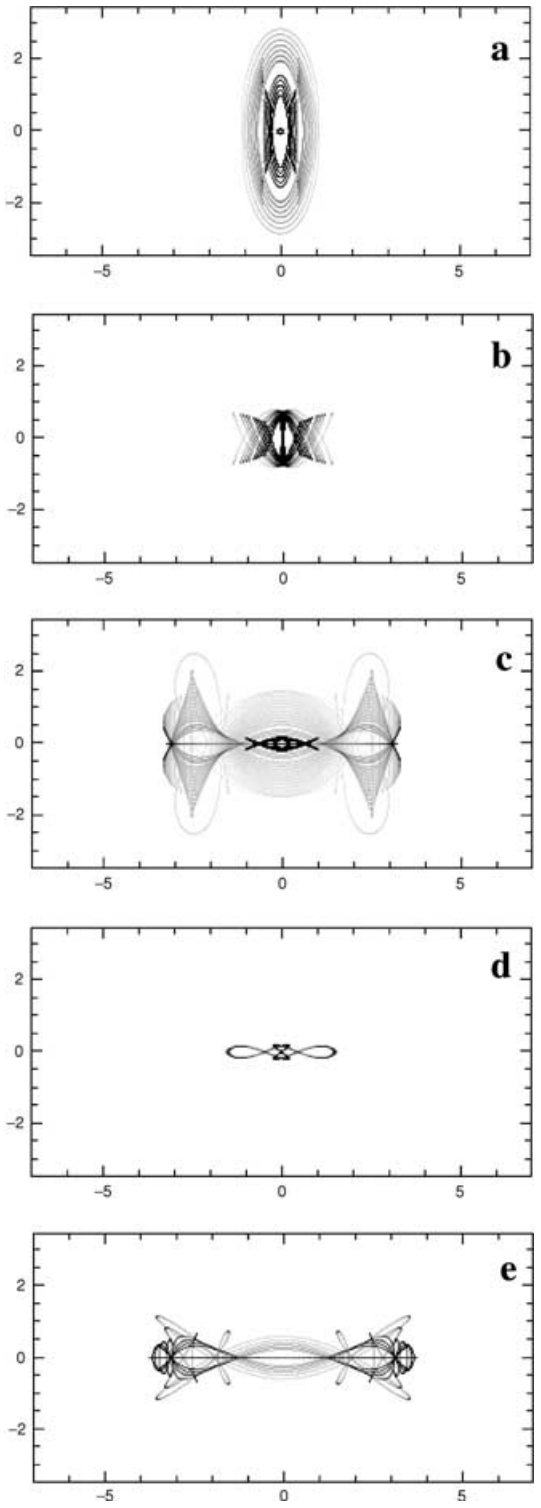

Figure 10. The end-on profiles of the families of model D. The layout is as in Fig. 9.

(or all orbits of a family) populated. Internal and external factors, like resonance widths, formation history, influence of companions etc. decide which of them will be populated in a real galaxy. For example, in Fig. 11(a) a boxy bulge could be built inside the 'borders' indicated by arrows, which are imposed by the x1v1 orbits. However, if for some reason x1v1 is not populated and the bar, apart from the stable members of the 2D x1 orbits, is made out of the families x1v4, x1v7 and x1v9, we have again a b/p profile, as we see in Fig. 11(b). The main difference between the two configurations, that would reflect in the photometry of edge-on galaxies, is the $B_{\rm L}/O_{\rm Ly}$ ratio or a similar indicator. In the present case a boxy bulge due to the x1v1 family would give $B_{\rm L}/O_{\rm Ly} \approx 2.1$, while the profile that is dominated by x1v4 has $B_{\rm L}/O_{\rm Ly} \approx 1.3$.

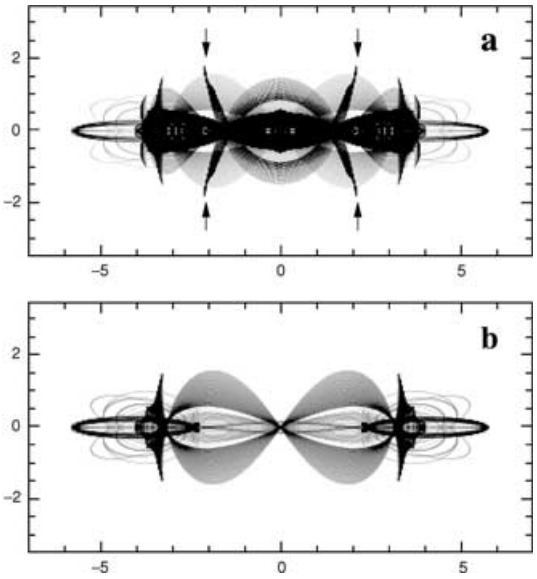

Figure 11. Composite side-on, (y, z), vertical profiles of model A1. (a) All 3D families except the banana-like orbits are considered. (b) The profile consists of families x1v4, x1v7 and x1v9.

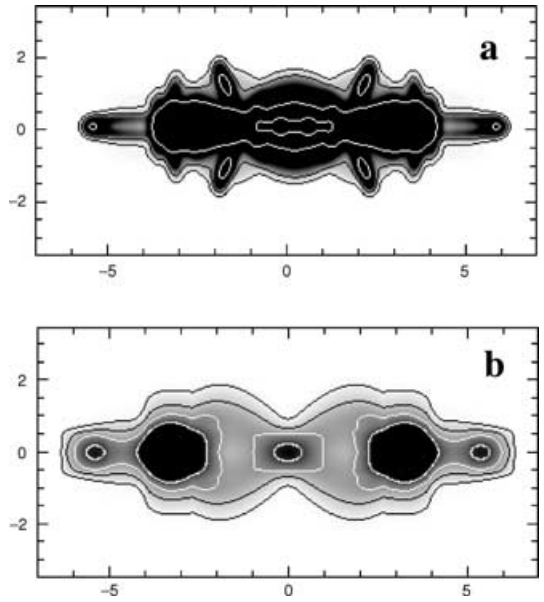

Figure 12. Blurred images of the side-on profiles given in Fig. 11. Characteristic isodensity contours indicate the morphologies which will be favoured to appear in model A1.

The family bifurcated from x1 at lowest energy, if populated, will characterize qualitatively the boxiness of a model's profile, because it determines whether we will have a peanut, a boxy, or a flat edge-on profile. The reason for this is that the orbits of a 3D family which bifurcated from x1 at a n : 1 vertical resonance, have in general larger $\overline{|z|}$ than the orbits of the family bifurcated at the $(n + 1)$: 1 vertical resonance. The family x1v3 can be an exception to this rule in some models (e.g. model A1), if it undergoes an S $\rightarrow \Delta$ transition when its orbits are still confined close to the equatorial plane without becoming stable for larger energies. This stability behaviour, however, has been encountered only in specific models and is not the general rule. In our models we found profiles whose vertical extent decreases as we move away from the centre of the galaxy. They present relatively abrupt height changes at distances from the centre which are characteristic for each family. So, the orbits of a given family reach a maximum distance from the centre along an axis. This is especially discernible in the case of the x1v1 family. These 'stair-type' edge-on profiles have been encountered in 3D spiral potentials (Patsis & Grosbøl 1996) and in almost axisymmetric disc models as well (Patsis et al. 2002a).

Blurred smoothed images are another informative representation of the profiles. They are created by applying a gaussian smoothing filter on the images using the corresponding MIDAS command. The smoothing radius, i.e. the number of pixels 'around' each central pixel, is 9 in both directions of the image. So we have a 19×19 pixels smoothing neighbourhood. The mean and sigma values that have been used are 9 and 6 pixels respectively, again in both directions. In order to construct exact density maps we would need self-consistent models based on libraries of non-periodic orbits (e.g. Schwarzschild 1979; Pfenniger 1984b; Contopoulos & Grosbøl 1988). This is beyond the scope of the present paper. Blurred images, however, show, in a first approximation, the coarse morphological features which are expected to be discernible in models made out of non-periodic orbits, trapped around the stable periodic ones. Thus our blurred images should not be considered as exact, but just as guiding the eye, for morphological features to be sought in the observations. We did not include in our blurred images planar orbits, which would appear just as thick straight-line segments on the equatorial plane.

The blurred images of the profiles of Fig. 11 are given in Fig. 12. We clearly see that we have boxy profiles both in (a) and in (b). The typical peanut morphology is better reproduced in Fig. 12(b) indicating that it is the x1v4 family that is mainly responsible for this morphology. On the other hand, the boxy structure in Fig. 12(a) (as the overplotted isodensities also show) is characterized by a local maximum height at $y = 0$. We note that families associated with vertical n : 1 resonances with $n > 4$ have little, if any, contribution to the vertical structures that dominate and characterize the profiles.

Fig. 13 is the end-on composite profile of model A1, considering all the families, as in Fig. 11(a). Its blurred image (Fig. 13b)

Table 6. Properties of edge-on profiles in model D. The columns are as in Table 1.

Model name	GM_D	GM_B	GM_S	ϵ_s	Ω_b	E_j (r-IILR)	E_j (v-ILR)	R_c	B_L	Comments
D	0.72	0.2	0.08	0.4	0.0540	−0.467	−0.440	6.31	5.7	Strong bar

Family	Initial conditions	B_L/O_{Ly}	s/o shape	R_{cor}/O_{Lx}	e/o shape	Comments
x1v1	$(x, z, 0, 0)$	2.4	⋈/X	6.3	⋈	
x1v3	$(x, z, 0, 0)$	1.2	⋈	4.9	×	
x1v5/x1v5′	$(x, z, 0, 0)$	1.2	⋈	1.9	⋈	
x1v6	$(x, 0, 0, \dot{z})$	1.0	⋍	4.2	⋈	
x1v7	$(x, 0, 0, \dot{z})$	1.2	⋍	1.7	⋈	

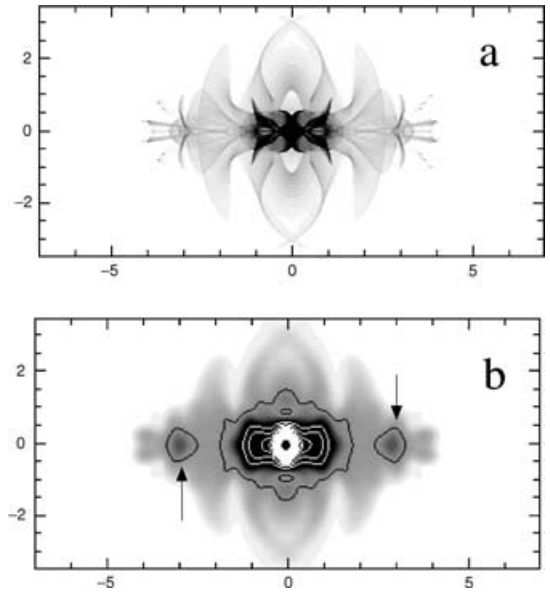

Figure 13. Composite end-on, (x, z), vertical profiles of model A1. (a) All 3D families of Fig. 11(a) are considered. (b) The blurred image of (a) (see text). The arrows point to the local density enhancements on either side of the boxy bulge.

clearly shows that also the (x, z) profile has a boxy character, as the (y, z) one. Now the box, as expected, is confined closer to the centre. Isodensity contours also in this case help understand the relative importance of the various features. The main contribution to the central dark box in Fig. 13(b) comes from the orbits of the x2-like 3D family of multiplicity 2 (Fig. 2g). We note that in the corresponding side-on profile the contribution of this family to the overall morphology is minimal, due to the confined extent of their (y, z) projections (they are elongated along the minor axis of the bar). Note the two surface density enhancements, symmetric with respect to the centre, indicated by arrows.

Model A2, the slow rotating bar case, gives a characteristic example of a well defined b/p shape due to successive orbits of the x1v1 family (Fig. 3b). Furthermore, it also gives a typical example of an 'X' morphology resulting from the superposition of successive orbits. The main reason for the sharpness of the 'X' feature is that the $S \rightarrow \Delta \rightarrow S$ transition of the x1v1 family in this model practically does not interrupt the succession of the stable orbits we consider, as x1v1 is complex unstable only over a very narrow energy interval. In this way the 'X' feature would be due to orbits trapped around the x1v1 family, rather than to orbits trapped around families of stable orbits on inclined orbital planes symmetric with respect to the rotational axis. The imprint of the 'X' in model A2 is given in Fig. 14(b). Note that the sides of the 'X' emerge out of a boxy feature in the very centre of the galaxy. Inspection of Fig. 3(b) explains the origin of this morphology. In the particular case of model A2, in the very inner part we also have the contribution of family x2v1 with orbits with similar weights as those of x1v1. Because of these, the 'X' feature does not extend with equal intensity all the way to the centre, unless the x2v1 are little populated. Note that an 'X' feature like the one presented by Whitmore & Bell (1988) (their Fig. 4) is passing through the centre and has equal intensity along its sides. Combining the profiles of x1v1 and x2v1 with those of x1v3 and x1v4, we obtain an edge-on profile of model A2 which has a striking similarity with the edge-on galaxy IC 4767 (Fig. 14a). We point with arrows at the enhancements of the surface density along the major

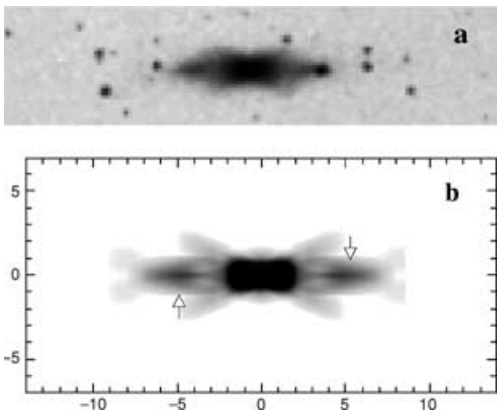

Figure 14. (a) DSS image of IC 4767 in *B*. (b) the side-on, (y, z), profile of model A2 made of the coexistence of the families x2v1, x1v1, x1v3 and x1v4. The arrows point to the local density enhancements on either side of the boxy bulge.

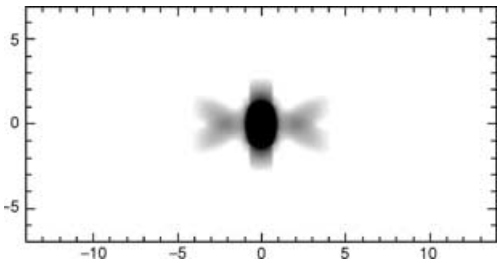

Figure 15. Composite end-on, (x, z), profile of model A2 given as a blurred image. The profile is build by the same families used in Fig. 14(b).

axis in Fig. 14(b). They clearly have their counterparts in the image of the galaxy (Fig. 14a) and are clearly revealed in the processed image in Whitmore & Bell (1988, their Fig. 1c).

Let us now turn to the end-on view of model A2 (Fig. 15). The family x2v1 contributes a cross-type end-on profile. The remaining families contribute mainly to the building of a dark bulge at the centre, which is slightly elongated along the rotational z axis. However, in this case corotation is at $r = 13.24$, so we have, even by considering x2v1, a ratio $R_{\rm cor}/O_{\rm Lx} \approx 3.6$, i.e. such features should be sought in the very central regions of end-on views of the discs of barred galaxies.

The fast rotating bar of model A3 offers an example, where the (y, z) profile is rather flat (Fig. 16a), mainly due to the complex instability of the x1v1 family. The *end-on* profile is in this case boxy (Fig. 16b). The boxiness is introduced by the families x1v3 and x1v5.

Model B, without either radial or vertical 2 : 1 resonances, offers many possibilities of showing a strong b/p feature if we consider all families that may contribute to its vertical profile. It even has a '⊃⊂' feature in its central part when viewed side-on (Fig. 17a). Note that in this case x1v1 orbits do not exist, as the first vertical bifurcation in model B is x1v5 introduced in the vertical 4 : 1 resonance (Paper II). The profile is made out of x1v5, x1v5′, x1v7 and z3.1s orbits, which give the '⊃⊂' morphology in the centre. Blurred images are given in Fig. 17(c) and Fig. 17(d) for the profiles in Fig. 17(a) and Fig. 17(b) (end-on view), respectively. The morphological difference between the x1v1 'X' and the z3.1s 'X', is that the latter is characteristically curved (i.e. it can be better described with the symbol '⊃⊂'), while the sides of the former are straight. The overplotted isophotes on the blurred images in Figs 17(c) and (d) reveal a peanut and a boxy

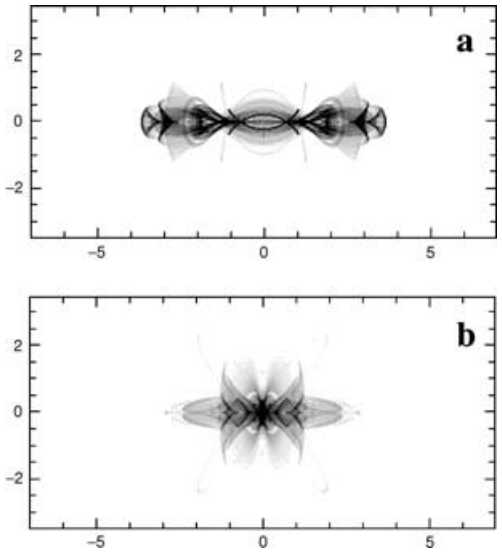

Figure 16. Composite profiles of model A3. (a) (y, z). (b) (x, z).

profile respectively. From Figs 7 and 17 it is evident that the families x1v5, x1v5′ support a boxy structure elongated along the major axis with, in the outer parts, an ansae-like morphology. On the other hand, the outer isophotes of z3.1s support the typical peanut morphology, while closer to the equatorial plane the isophotes have the kind of b/p shape encountered in several 3D bars of *N*-body models (Athanassoula, private communication).

In Fig. 18 we give in blurred representation also the edge-on (18a) and end-on (18b) profiles of the x1v1 family in model C. In both figures we have considered even orbits that reach $|z| > 1.5$, in order to show that the x1v1 orbits do not contribute to the observed boxy feature beyond the critical energy for which they start to increase their mean radii by increasing practically only their mean $|z|$ values. Beyond the dashed lines, away from the equatorial plane, the corresponding density is too low. We see that a bar with such a family as backbone supports a peanut edge-on and a boxy end-on profile, and also that we have here a case where the x1v1 family supports the 'X' feature in its central morphology.

Finally, in model D (Fig. 19) we have another case characterized by the dominance of x1v1. This family brings in the side-on morphology a b/p bulge and broken branches of a 'X' feature. The end-on profile of this model gives a rather roundish or rhomboidal central feature, which becomes elongated in the z direction if we take into account orbits with mean $|z| > 1.5$ (Fig. 19d).

5 DISCUSSION

In this paper we have investigated families of periodic orbits, as well as combinations of such families, that might be the building blocks for b/p edge-on morphologies in disc galaxies. The B_L/O_{Ly} ratios in the side-on views of the models vary. Profiles with B_L/O_{Ly} ratios of less than 2 characterize models in which most of the material of the bar forms a b/p structure. On the other hand, in cases with big B_L/O_{Ly} ratios we have to deal with b/p features concentrated close to the centre of the model. In almost all cases (except for the z3.1s family) the orbits that contribute to a b/p profile are introduced in the system as bifurcations of the basic family x1 at vertical resonances. For this reason we used orbits of these families in building possible orbital profiles.

In our study we present the orbital profiles as viewed from the two extreme edge-on viewing angles, namely the side- and the end-on view. Possible changes in the morphology of the profiles due to rotation have been discussed in Section 3.1. There, we investigated the role of rotation in minimizing the effect of the presence of the third local maximum in the profiles of the x1v1 family in model A1. We concluded that the morphological change from a structure with three local maxima to a kind of 'X'-feature happens only for a small angle range. We find in general that the profiles keep their morphological similarity with their side-on views for viewing angles close to it, and the same happens with the end-on projections. If we rotate a b/p profile around the axis of rotation of the system, starting from the side-on view, we observe that the local minimum at its centre rises above the equatorial plane and the profile becomes 'thicker' at the centre. This, however, does not affect the overall

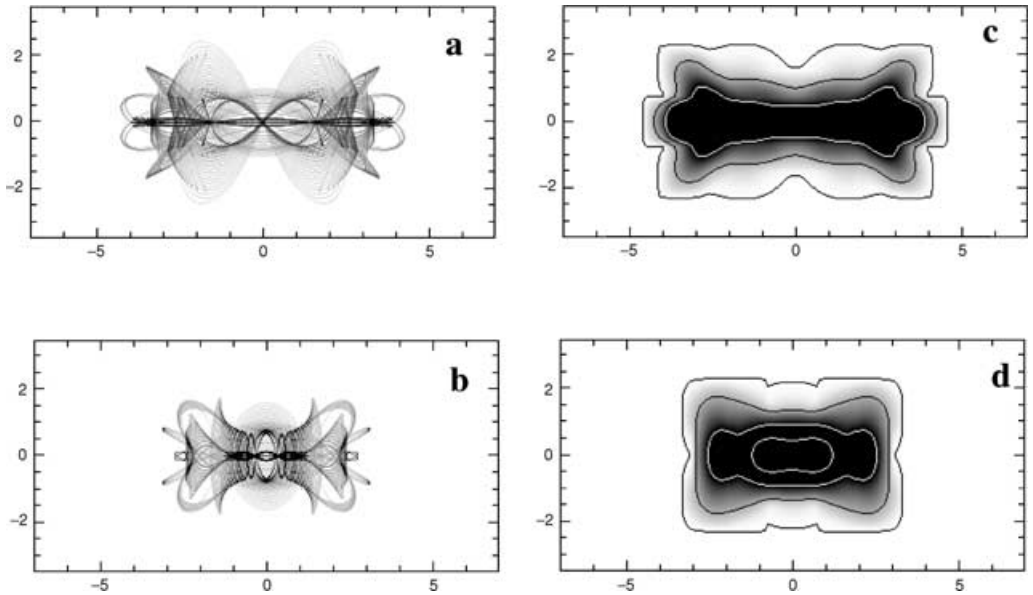

Figure 17. Composite profiles of model B made out of x1v5, x1v5′, x1v7 and z3.1s orbits. (a) (y, z). (b) (x, z). In (c) and (d) are given the blurred images of (a) and (b), respectively. Characteristic isodensity contours indicate the morphologies which will be favoured to appear in model B.

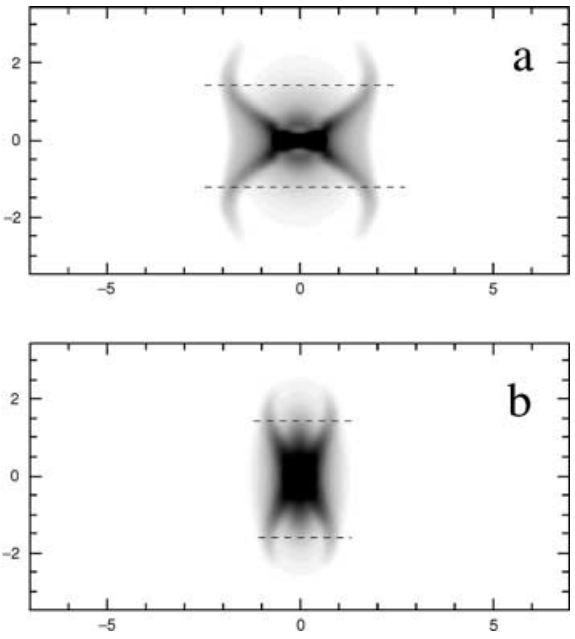

Figure 18. Blurred representation of the side-on (a) and end-on (b) profiles of the x1v1 family in model C. The dashed lines indicate the region beyond which x1v1 orbits contribute to the local density only by orbits growing their sizes in $\overline{|z|}$ without increasing their projections along the major axis.

morphology of a b/p structure. We note that in blurred images of side-on projections, this minimum does not reach the equatorial plane (Figs 12b and 14b). Nevertheless, the size of the bar altogether varies in different projections.

Lütticke et al. (2000b) hold the view that the inner regions of barred disc galaxies, apart from the thin bar, are built by two further components, namely a spheroidal bulge and a b/p structure. The spheroidal is a kinematically distinct component occupying the central region of the galaxy. Our models do not exclude the coexistence of spheroidals in the central regions of the discs. Furthermore, we find families of periodic orbits in the x1-tree, i.e. families of the 3D disc, that could support roundish structures, especially in their end-on projections. It is also possible, as we found z3.1s, to find a plethora of 'z*n*' families that stay close to the rotational axis and could populate a spheroidal bulge (e.g. family z5.1s given in fig. 13 of Paper II). These orbits are not presented in this paper, as we only discuss here the presence and morphology of peanuts or boxes. Peanuts and boxes are structures associated with families of the bar, or, more generally, with families of the disc, as they can also exist in almost axisymmetric models (Patsis et al. 2002a), as well as in the case where instead of a bar we have a spiral perturbation (Patsis & Grosbøl 1996). Note also that the z3.1s family is bar-supporting (Paper II).

Peanuts made out of the x1v1 family (i.e. related to the vertical 2 : 1 resonance) and in which orbits beyond the $\Delta \rightarrow$ S transition are populated show a spheroidal structure in the middle, which introduces a third local maximum at the centres of the side-on profiles. The central empty region of the '○' feature is surrounded by parts of x1v1 orbits. Branches of a 'X' are stuck in several cases to the left and to the right of this spheroidal structure. We can clearly see it in Fig. 11(a), between the features pointed with arrows, and also in the corresponding position of the edge-on profile of the strong bar model D (Fig. 19a). In these cases the ratio of the extent of the central pseudo-bulge over the extent of the peanut-shaped structure is almost 1.

Geometrical arguments are also useful when comparing b/p features of real galaxies or b/p features encountered in *N*-body simulations with b/p structures in our orbital models. Unfortunately the various lengths involved are measured in different ways by different authors. Usually the way of measuring a length is intrinsic in the approach adopted by the authors in order to study edge-on profiles. Thus a direct comparison is problematic.

The peanut- or box-like features we find in the composite side-on profiles have $B_{\rm L}/O_{\rm Ly}$ ratios which vary from about 2.5 to close

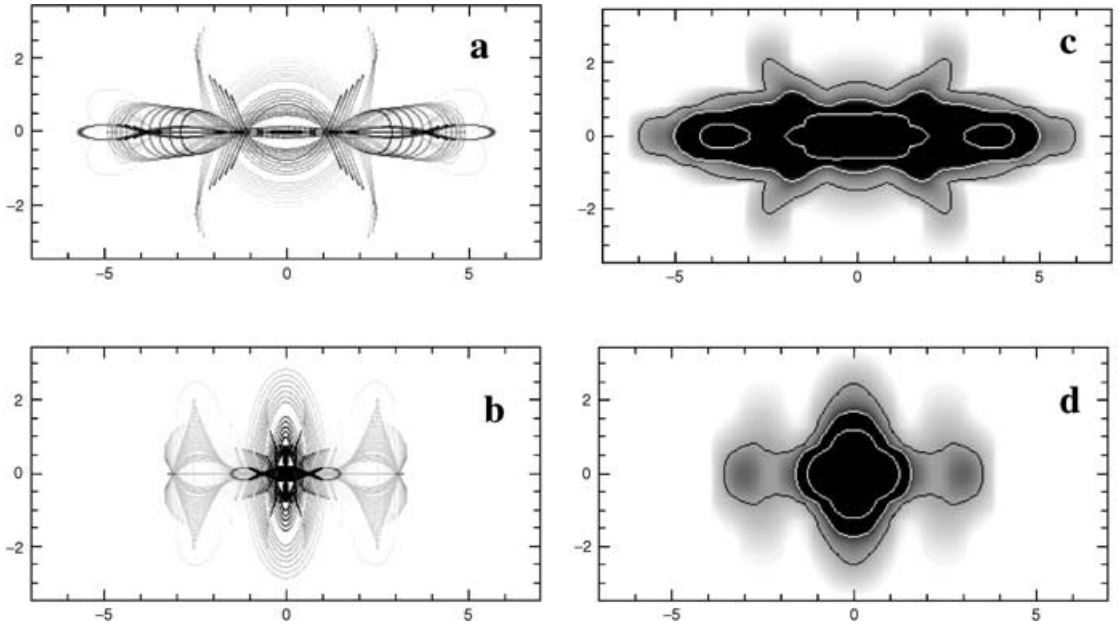

Figure 19. Composite profiles of model D with a strong bar. (a) (y, z), (b) (x, z), (c) blurred (y, z) and (d) blurred (x, z). In panels (c) and (d) we include isocontours characteristic of the morphology of this model. It is evident that strong bars are associated with b/p side-on profiles and favour the presence of an 'X' feature.

to 1. In our measurements the length of the bar B_L is the length of the longest projection of bar-supporting orbits on the semi-major axis. In general these are x1 orbits with loops on the major axis of the bar, or 2D rectangular-like orbits at the radial 4 : 1 resonance region (Paper IV). Thus, an upper limit to this length is defined in a rather precise way. On the other hand, the orbital length along the major axis, O_{Ly}, can not exceed the length of the projection of the outermost orbit of a family on the semi-major axis, but it can in principle take smaller values, depending on whether all or part of the family is populated in the profile we construct. In that sense the B_L/O_{Ly} ratios we give can be considered as minimum values for a profile dominated by a specific family, as we usually exclude only orbits that reach big heights above the equatorial plane, which do not contribute much to density profiles anyway. Nevertheless, if a family characterizes a profile this means that the majority of its orbits is populated and in this case the ratio cannot be considerably larger than the number we give.

By taking all the above into account we could compare the ratios we find with corresponding quantities defined in Athanassoula & Misiriotis (2002). This paper quantitatively examines morphologies found in *N*-body models of barred galaxies. In an edge-on projection they estimate the extent of the bar and of the b/p feature by considering cuts of the projected surface density parallel to the equatorial plane. In the simulations where they find a strong b/p feature, the ratio of the maximum distance to which the ledge on the $z = 0$ cut extends to the radius of very steep drops on cuts offset from $z = 0$, is ≈ 1.5. This points to profiles dominated by orbits of families like x1v3, x1v4 or x1v5, which in their side-on profiles have B_L/O_{Ly} ratios less than 2. Despite the differences that can be introduced due to the different kind of modelling and the different ways of estimating the various relative lengths, the b/p features in Athanassoula & Misiriotis (2002) definitely occupy regions larger than the central region of the galaxy. This indicates that a large fraction of the bar seen side-on has a b/p morphology.

Lütticke et al. (2000b) find in their sample a ratio around 2.5 for the bar length over the b/p distortion (BAL/BPL). Here again we have to note the differences in the way they estimate the length of the bar and the length of the b/p structure. As in Athanassoula & Misiriotis (2002) they consider cuts parallel to the equatorial plane of edge-on disc galaxies. The projected bar length, however, is estimated in the cut along the major axis at the distance where they find an increasing light distribution towards the centre compared to the radial exponential light distribution. The length of the b/p structure is defined as the distance between the maxima of the b/p distortion. Therefore, their bar length is systematically larger than both our B_L and the bar length estimated in Athanassoula & Misiriotis (2002). Also BPL in Lütticke et al. (2000b) is systematically smaller than our orbital length O_{Ly}, because for most families parts of the orbits also extend to the left and to the right of the maxima of the b/p feature. An exception is family x1v1 for which the distance between the b/p maxima and the length of the projection of the orbital profile on the semi-major axis indeed almost coincide (see e.g. Fig. 1a). As a result of all the above mentioned differences the BAL/BPL ratio in Lütticke et al. (2000b) is expected to be systematically larger than our B_L/O_{Ly} in profiles dominated by the same family. For our models ratios around 2.5 point to x1v1 type peanuts or, in models without radial and vertical ILRs, to peanuts that are made of z3.1s orbits. This, however, does not exclude that many galaxies in the Lütticke et al. (2000b) sample could have B_L/O_{Ly} less than 2 for the family which is mainly responsible for its vertical profile.

As a general rule we can say that, if the relative size of a b/p feature compared with the size of the bar is estimated smaller than 2, this indicates that most probable candidates to be associated with it are families related to higher order vertical resonances (e.g. x1v3, x1v4 etc.) and not the x1v1 family. The main reason for this is that the x1v1 orbits, as energy increases approaching corotation, do not increase their projections on the major axis of the bar after a critical energy. Beyond this energy, the x1v1 orbits grow practically only in z.

For cases of edge-on galaxies where the ratio of the bar to the b/p distortion's length is larger than 3, the orbital models indicate that these features may be associated with nearly end-on projections of various families (see Figs 2b and g, Figs 6b and c, Fig. 10b). Also existing x2-like 3D orbits would contribute to boxy end-on profiles. x1v1, the family associated with the vertical 2 : 1 resonance, does not give boxy end-on projections. It contributes rather to a roundish central morphology (Figs 1a, 9a and 19d). At this point we want to stress that side-on b/p profiles combined with slightly prolate end-on morphologies, as well as boxy, or even b/p, end-on profiles are encountered in 3D bars in *N*-body simulations (Athanassoula 2002, private communication).

Another feature that we can geometrically quantify is the oblique angle between a branch of 'X' and the major axis of the main bar. In the slow bar model A2 the 'X' is made mainly of the x1v1 orbits and this angle is about 27° (Fig. 3b), close to the value Whitmore & Bell (1988) give for IC 4767. The x1v1 orbits of models A1 (fiducial case) and D (strong bar case) harbour 'X's embedded in peanut-shaped bulges, which are characterized by the fact that they do not reach the major axis. As we explained, this results from the presence of the complex unstable part of this family which causes an empty inner region. In these cases the angle is about 50°. In the strong bar case (model D) the peanut feature with an 'X' is particularly conspicuous, in agreement with the results of *N*-body simulations (Athanassoula & Misiriotis 2002; Athanassoula, private communication). The central '⊃⊂' feature made out of the z3.1s orbits in the model without 2 : 1 resonances does not include segments with straight lines. However, tangents crossing through the centre are inclined about 43° to the major axis. We can define an inner and an outer inclination for branches of the '⊃⊂' features due to the x1v4 family that might appear in several models. In model A1 we measure this to be about 25° if we consider stable x1v4 orbits with low energy, and 50° if we consider stable x1v4 orbits with large energies (Fig. 11b). A rough estimation of the angle of 'X' in Hickson 87a from fig. 4 in Mihos et al. (1995), is about 30°. Lütticke et al. (2000c) estimate this angle to be $40° \pm 10$. To summarize, small 'X'-angles' ($< 30°$) are build from orbits related to families introduced at higher order vertical resonances and to some degree slow rotating bars, while large 'X'-angles' ($> 40°$) characterize 'X' structures in typical x1v1 b/p bulges.

The overlapping of periodic orbits of some families form two enhancements of the projected surface density along the major axis of the models, which are symmetric with respect to the centre. Similar features, seen along the major axes of edge-on disc galaxies with b/p bulges, e.g. IC 4767 (Whitmore & Bell 1988), ESO 417-G08, NGC 4710 (Schwarzkopf & Dettmar 2000) are often interpreted as rings or spirals. Here we present an alternative explanation. Using families of periodic orbits as building blocks of the profiles of the edge-on barred galaxies we can easily see that the enhancements could be a kind of a projection effect due to the trapping of material around stable periodic orbits. These enhancements actually exist in the profiles of all families. In composite profiles one can better see them at families with orbits close to the end of the bar. The reason is that there are no other families of periodic orbits that fall on them smoothing out the profile more. Recently Aronica et al. (2002, and

in preparation), detected these enhancements in a sample of edge-on galaxies observed in the K′.

We note that we found b/p features in models without a radial 2 : 1 resonance (model C, cf. Fig. 18) and that we encountered a case (model A3) where although the radial and vertical 2 : 1 resonances exist and are located at very close energy values (Paper II), the model does not support a conspicuous b/p structure (cf. Fig. 5). Thus in our response models we do not find any correlation of a conjunction of radial and vertical 2 : 1 resonance and the appearance of a b/p feature.

Finally our models could support small inner discs, tilted with respect to the equatorial plane of the main disc. This can be done by breaking the symmetry and considering only one of the symmetric branches of a family. In galaxies this can be e.g. due to companions falling on a target galaxy at a skew angle, so that the system will show a preference in populating one of the two symmetric branches.

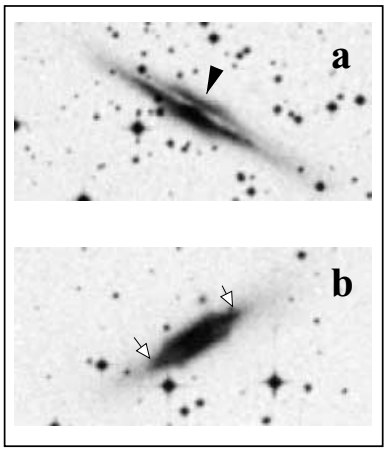

Figure 20. DSS images of NGC 2788 A (a), and NGC 6771 (b). Both galaxies show a b/p profile.

6 CONCLUSIONS

In this paper we investigated the vertical structure in barred potentials using orbital theory. We combined families of periodic orbits in the models of Papers I and II in order to study the possible resulting vertical profiles and we discussed their geometry and their dimensions in comparison with structures found in edge-on disc galaxies and snapshots of *N*-body simulations. Here we list our basic conclusions as follows.

(i) The vertical profiles of our models are of 'stair-type'. This means that families that offer the skeletons for the 3D bars and are bifurcated at higher energies (i.e. closer to corotation) have in general lower mean heights.

(ii) b/p features in vertical profiles can be supported mainly by the families listed as follows. (a) **x1v1**. This family is particularly useful for building a boxy central structure if it does not have a complex unstable part in the critical energy. The best examples we found are in the slow rotating bar case and in the strong bar model. In these cases, for energies where the maximum z of the orbits remains less than about 1 kpc, successive orbits of x1v1 have the maximal deviations of their edge-on projections from the equatorial plane aligned along almost straight segments. These 'lines' are in oblique angles to the major axis, not passing thorough the centre in general, and their angle with the major axis is $\approx 50^\circ$. In the slow bar case, however, this angle is $\approx 27^\circ$. For this family the ratio B_L/O_{Ly} *is larger than 2*. $B_L/O_{Ly} > 3$ for x1v1 (as found in model A3), indicate that only a small part of the family is populated and thus its contribution to the vertical structure of the model is not significant. (b) **x1v4**. This family gives $B_L/O_{Ly} \approx 1.3$, i.e. brings the end of the peanuts close to the end of the bars. It is introduced in the system after a U $\rightarrow$ S transition of x1 and has stable representatives for larger energies than the energy at the bifurcating point. It exists over large energy intervals and, if populated, will provide the system with a b/p-shaped structure whose extent is near that of the bar. It supports the peanut morphology, especially in composite profiles without any contribution from x1v1 orbits (Fig. 12b). (c) **z3.1s**. This family gives b/p features in models without radial or vertical ILRs, and is quite important for the dynamics of these models. Profiles characterized by the presence of this family (Figs 17c and 7c) have the characteristic local minimum of the density at the (0, 0) position, like in the case of NGC 2788 A in Fig. 20(a), which is indicated by a black arrow. (d) The ansae-type profile is easiest made by orbits associated with the vertical 4 : 1 resonance and can be described as a stretched 'X' (Fig. 7a). (e) Finally, the 3D **x2-like** families of orbits support boxy morphologies. The latter are especially discernible in the end-on profiles of the model with the low pattern speed.

We have to note that if families bifurcated at high order vertical resonances are responsible for the peanut, then they will support a b/p bar morphology altogether. Coexistence of several 3D families should in general be expected. In such a case it is the family which is bifurcated at the lowest energy that plays the most important role for the morphology of the model.

(iii) Narrow extensions appear on the sides of many profiles (see e.g. Fig. 12a) These features result from the 'stair-type' character of profiles constructed with families of periodic orbits, and have their counterpart in many images of edge-on disc galaxies. The corresponding feature in the case of NGC 6771 is also indicated by white arrows in Fig. 20(b).

(iv) The projection of the orbits of a family on the equatorial plane is confined within certain limits. By this we mean that moving on the characteristic towards corotation we reach a certain distance from the centre where the mean radius of the orbits increases only due to increasing of z. This is particularly evident in the case of the x1v1 family, which is related to the vertical 2 : 1 resonance and which in general is the 3D bifurcation of x1 closest to the centre.

(v) Families of periodic orbits (x1v3, x1v4, x1v5, z3.1s, x2v1) can build boxy, or even peanut-boxy, *end-on* profiles. We would thus like to suggest that boxy bulges in galaxies having a bar length over a b/p length larger than 3, are related with the profiles of families seen end-on.

(vi) 'X'-type features are found in the composite orbital profiles. They are formed by alignment of successive orbits of the family x1v1. They are pronounced if the S $\rightarrow$ Δ transition in this family does not play an important role in the dynamics of a model. The fact that 'X' features are rare in real galaxies, indicates that, in most cases where a x1v1 family is populated in a galaxy, it has an important complex unstable part. Adequate successive projections of the orbits of a family in large energy intervals, like what we see in model B mainly due to the z3.1s orbits, give central morphologies that can be described with the symbol '⊃⊂'. We note that the higher the order of the resonance of the family associated with 'X' or '⊃⊂' structure is, the smaller the angle between the 'X'/'⊃⊂'-branch and the major axis we find. In the case of the x1v1 family this angle is smaller in the slower rotating bar case.

(vii) Discs out of the equatorial plane in the bulges are easiest made by breaking the symmetry and populating only one of the two symmetric branches of the 3D families.

(viii) Characteristic local enhancements of the surface density along the major axis of the bar are predicted by the models merely due to the orientation of the successive orbits in the profiles.

ACKNOWLEDGMENTS

We acknowledge fruitful discussions and very useful comments by G. Contopoulos and A. Bosma. We thank the referee for useful suggestions and valuable remarks, which improved the paper. This work has been supported by ΕΠΕΤ II and ΚΠΣ 1994–1999; and by the Research Committee of the Academy of Athens. ChS and PAP thank the Laboratoire d'Astrophysique de Marseille for an invitation during which essential parts of this work have been completed. ChS was partially supported by the 'Karatheodory' postdoctoral fellowship No 2794 of the University of Patras. All image processing work has been done with ESO- MIDAS.

REFERENCES

Aronica G., Bureau M., Athanassoula E., Bosma E., Dettmar R. J., Vergani D., Pohlen M., 2002, in Hensler G., Stasinska G., Harfst S., Kroupa P., eds, The evolution of Galaxies III. From Simple Approaches to Self Consistent Models. Chr. Theis, in press
Athanassoula E., Bureau M., 1999, ApJ, 522, 699
Athanassoula E., Misiriotis A., 2002, MNRAS, 330, 35
Berentzen I., Heller C. H., Shlosman I., Fricke K. J., 1998, MNRAS, 300, 49
Binney J., Petrou M., 1985, MNRAS, 214, 449
Burbidge E.M., Burbidge G.R., 1959, ApJ, 130, 20
Bureau M., Athanassoula E., 1999, ApJ, 522, 686
Bureau M., Freeman K., 1999, AJ, 118, 126
Combes F., Sanders R. H., 1981, A&A, 96, 164
Combes F., Debbasch F., Friedli D., Pfenniger D., 1990, A&A, 233, 95
Contopoulos G., Grosbøl P., 1988, A&A, 197, 83
D'Onofrio M., Capaccioli M., Merluzzi P., Zaggia S., Boulesteix J., 1999, A&AS, 134, 437
Kormendy J., Illingworth G., 1982, ApJ, 256, 460
Kuijken K., Merrifield M. R., 1995, ApJ, 443, L13
Lütticke R., Dettmar R-J., Pohlen M., 2000a, A&AS, 145, 405
Lütticke R., Dettmar R-J., Pohlen M., 2000b, A&A, 362, 435
Lütticke R., Dettmar R-J., Pohlen M., 2000c, Astron. Gesell. Abs. S., Vol. 17, 68
Mihos J. C., Walker I. R., Hernquist L., 1995, ApJ, 447, L87
Patsis P. A., Contopoulos G., Grosbøl P., 1991, A&A, 243, 373
Patsis P.A., Grosbøl P., 1996, A&A, 315, 371
Patsis P. A., Athanassoula E., Grosbøl, Skokos Ch., 2002a, MNRAS, 335, 1049
Patsis P. A., Skokos Ch., Athanassoula E., 2002b, MNRAS, submitted (Paper IV)
Pfenniger D., 1984a, A&A, 134, 373
Pfenniger D., 1984b, A&A, 141, 171
Pfenniger D., 1985, A&A, 150, 112
Pfenniger D., Friedli D., 1991, A&A, 252, 75
Raha N., Sellwood J. A., James R. A., Kahn F. D., 1991, Nat, 352, 411
Schwarzkopf U., Dettmar R.-J., 2000, A&AS, 144, 85
Shaw M., 1993, MNRAS, 261, 718
Skokos Ch., Patsis P. A., Athanassoula E., 2002a, MNRAS, 333, 847 (Paper I)
Skokos Ch., Patsis P. A., Athanassoula E., 2002b, MNRAS, 333, 861 (Paper II)
Schwarzschild M., 1979, ApJ, 232, 236
Whitmore B. C., Bell M., 1988, ApJ, 324, 741
Zachilas L., 1993, A&AS, 97, 549

This paper has been typeset from a TEX/LATEX file prepared by the author.